# On the Multilayer Planning of Filterless Optical Networks with OTN Encryption

Qian Lv and Zuqing Zhu, *Fellow, IEEE*

***Abstract*—With enhanced cost-effectiveness, filterless optical networks (FONs) have been considered as a promising candidate for future optical infrastructure. However, as the transmission in FON relies on the "select-and-broadcast" scenario, it is more vulnerable to eavesdropping. Therefore, encrypting the communications in FONs will be indispensable, and this can be realized by introducing the optical transport network (OTN) encryption technologies that leverage high-speed encryption cards (ECs) to protect the integrity of OTN payload frames. In this paper, we study the problem of security-aware multilayer planning of FONs with OTN encryption. We first formulate a mixed integer linear programming (MILP) model (*i.e.*, w-MILP) to solve the problem exactly. Then, to reduce the time complexity of problem-solving, we transform w-MILP into two correlated MILP models for establishing fiber trees for an FON (t-MILP) and planning flows in the fiber trees (s-MILP), respectively. The optimization in t-MILP is further transformed into a weighted set partitioning problem, which can be solved time-efficiently. As for s-MILP, we propose a polynomial-time approximation algorithm based on linear programming (LP) relaxation and randomized rounding. Extensive simulations verify the performance of our proposals.**

***Index Terms*—Multilayer network planning, Optical transport network (OTN), OTN encryption, Physical-layer security, Randomized rounding, Approximation algorithm.**

## I. Introduction

NOWADAYS, the fast development of cloud computing and rasing of 5G communications have put great pressure on the underlying network infrastructure, especially the metro-aggregation segment [1, 2]. This stimulated intensive research and development (R&D) activities in a number of areas (*e.g.*, physical-layer technologies [3–5] and virtualization technologies [6–8]) to make networks more flexible. Meanwhile, as the main transport platform for large-capacity communications, optical networks are also looking forward to new architectures that can better balance the tradeoff between capacity and cost. In today's optical networks for the metro-aggregation segment, optical switching contributes to a significant part in the capital expenditures (CAPEX) and operating expenses (OPEX) [9]. Therefore, filterless optical networks (FONs) [10] have been proposed to minimize the need of optical switching for a more cost-efficient and energy-efficient optical infrastructure.

Since its inception [10], FON has been trying to replace optical filtering and switching elements (*e.g.*, reconfigurable optical add-drop multiplexers (ROADMs)) with passive splitters/combiners, for reducing CAPEX and OPEX. Note that, the removal of optical filtering and switching elements makes the transmission in FON rely on the "broadcast-and-select" scenario, which allows the optical signal that enters a filterless node to be broadcasted to all of its downstream neighbors. This, however, introduces security vulnerability, as a malicious party can tap into communications much more easily. Hence, encrypting the communications in FONs will be indispensable, especially for the cases where sensitive data is exchanged.

Q. Lv and Z. Zhu are with the School of Information Science and Technology, University of Science and Technology of China, Hefei, Anhui 230027, P. R. China (email: zqzhu@ieee.org).

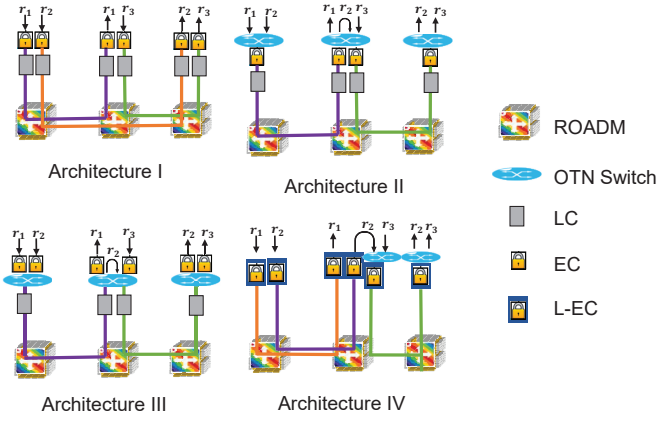


Fig. 1. Architectures for arranging the optical, packet and encryption layers in multilayer planning with OTN encryption (*Architectures* I-III adapted from [13], and *Architecture* IV derived from [14, 15])

Previously, to address the security issues in metro/backbone networks, people have developed optical transport network (OTN) encryption technologies that leverage high-speed encryption cards (ECs) to protect the integrity of OTN transmission [11]. Specifically, ECs provide a hardware-based encryption solution that can run certified cryptographic algorithms at OTN line-rates to encrypt the data in OTN payload frames. This is equivalent to adding a new encryption layer (*i.e.*, the ECs) to the original packet (*i.e.*, OTN line cards (LCs) and switches) and optical (*i.e.*, optical transmission and switching elements) layers of metro and backbone networks [12]. Hence, a few architectures have been proposed to arrange the network elements in the three layers and facilitate security-aware traffic grooming and wavelength routing [13–15].

As shown in Fig. 1, three architectures have been considered in [13], where *Architecture* I maps each packet flow $r_i$ to a bundle of EC and LC at its transmitter or receiver side and sets up an end-to-end lightpath between the LCs to transmit the flow, *Architecture* II grooms multiple flows to a bundle of EC and LC and can use multi-hop lightpath routing to transmit a flow, and *Architecture* III encrypts each flow with an EC, grooms the encrypted flows to an LC, and can also transmit a flow with multi-hop lightpath routing. Lately, with

the advances in system integration, people have fabricated the full-rate line-encryption cards (L-ECs) [14, 15] that can cover the functionalities of both EC and LC (*i.e.*, OTN encryption and OTN transmission), and each L-EC can replace a bundle of EC and LC when the capacities are the same. Therefore, L-ECs can better utilize the slots in each chassis and realize simpler network control and management (NC&M), and moreover, due to the system integration, the cost of an L-EC is lower than that of a bundle of EC and LC, when the capacities are the same [14, 15]. Meanwhile, the introduction of L-ECs provides operators with more options to provision their flows (as shown in the *Architecture* IV in Fig. 1), with which the CAPEX of security-aware multilayer planning can be saved [16].

After introducing the encryption layer and considering the architectures in Fig. 1, the multilayer planning of a packet-over-optical network can be much more complex than that of one without OTN encryption [12]. This is because we need to first consider the security requirement of each packet flow (i.e., whether its routing path goes through untrusted zones) to determine whether it needs to be encrypted, and then select proper architecture(s) from *Architectures* I-IV to provision it with the minimum cost. Moreover, the network planning of FONs is fundamentally different from that of conventional optical networks, since we need to divide the physical topology of fiber connections into a set of fiber trees to avoid causing laser-loop effects due to continuous signal broadcasting and amplification [17, 18]. Fig. 2 illustrates an example on the network planning of FONs. Specifically, we divide the physical topology in Fig. 2(a) into two link-disjoint fiber trees, which are denoted with green-dashed and red-solid lines in Fig. 2(b), respectively. It can be seen that each fiber tree does not contain any loop. Meanwhile, the optical signal from any node on a fiber tree is broadcasted to all the other nodes on the fiber tree, while if two nodes are not on a same fiber tree, they cannot talk with each other directly in the optical layer (*i.e.*, the communications between them have to be relayed in the packet/encryption layers at a common node of their fiber trees).

For instance, in Fig. 2(b), the signal of the lightpath from *Node* 2 to *Node* 7 can also be received by *Nodes* 3-6 on the same fiber tree, and among them, *Node* 3 is not trusted by *Node* 2. Therefore, the flow(s) on the lightpath should go through the encryption layer before entering the optical layer. To this end, we can see that the security-aware multilayer planning of FONs with OTN encryption is even more challenging than its counterpart for a conventional packet-over-optical network. To the best of our knowledge, this problem has not been studied in the literature, except for our preliminary work on it in [16].

In this paper, we greatly extend our preliminary work in [16] to study the security-aware multilayer planning of FONs with OTN encryption comprehensively. Specifically, we make the following major improvements. Firstly, we jointly consider *Architectures* I-IV and add several new constraints (*i.e.*, flows cannot be decrypted on untrusted nodes, and each lightpath can only be transmitted in a fiber tree within a maximum hop-count (for approximating the reach constraint of the lightpath)), to improve the practicalness and completeness of our network model. Secondly, we not only formulate an overall MILP model (*i.e.*, the w-MILP) to solve the problem exactly, but also transform w-MILP into two correlated MILP models (*i.e.*, the t-MILP and s-MILP) for establishing fiber trees and provisioning flows in the fiber trees, respectively. Thirdly, we optimize the formulation of t-MILP to make it more compact, such that the subproblem of establishing fiber trees can be solved quickly. Fourthly, we propose a novel polynomial-time approximation algorithm based on linear programming (LP) relaxation and randomized rounding to solve s-MILP, and prove that it can provide probabilistic guarantee of a bounded approximation ratio. The major contributions of this work are:

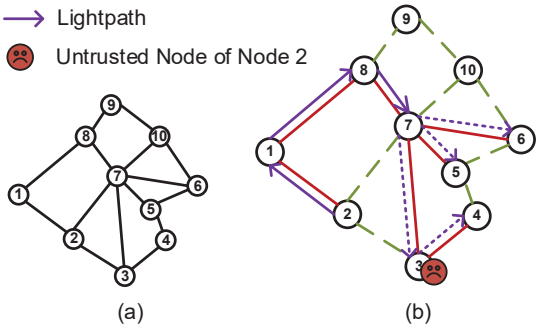


Fig. 2. Example on network planning of an FON, (a) Physical topology, and (b) Establishment of fiber trees.

- To the best of our knowledge, we are the first to study the problem of security-aware multilayer planning of FONs with OTN encryption comprehensively.
- We formulate the w-MILP to solve the problem exactly, and propose to divide it into two subproblems and solve them sequentially for near-optimal solutions.
- We show that the first subproblem on the establishment of fiber trees can be transformed into the classic weighted set partitioning problem and solved accordingly.
- For the second subproblem on the allocation of LCs/ECs/L-ECs, we design a polynomial-time approximation algorithm, and prove that it can provide probabilistic guarantee of a bounded approximation ratio.
- We conduct extensive simulations to evaluate our proposals and confirm their effectiveness.

The rest of the paper is organized as follows. Section II surveys the related work briefly. The problem description and the w-MILP of security-aware multilayer planning in FONs with OTN encryption are presented in Section III. We show the algorithm design in Section IV, including transforming w-MILP to t-MILP and s-MILP and proposing the approximation algorithm for s-MILP. The numerical simulations are discussed in Section V. Finally, Section VI summarizes the paper.

## II. Related Work

The multilayer planning of a packet-over-optical network generally includes grooming the traffic from the packet layer, planning lightpaths to carry the aggregated traffic, and calculating the routing and spectrum assignment (RSA) for the lightpaths. There have been many studies on the multilayer planning problem, considering different optical layer technologies and various traffic demands [19–26]. Among them, the studies in [25, 26] considered the multilayer planning of FONs

with point-to-multipoint coherent transceivers. Meanwhile, it is known that optical networks are vulnerable to physical-layer attacks [27]. Thus, previous studies in [28–30] proposed a few security-aware planning algorithms to arrange the RSA of lightpaths such that physical-layer vulnerabilities can be minimized. However, none of these studies have considered the security-aware multilayer planning with OTN encryption.

Guan *et al.* [13] first laid out three architectures that can be used in multilayer planning with OTN encryption. The authors of [31] evaluated the performance of these architectures in the situation where multilayer restoration needs to be invoked to address outages in the packet layer. Recently, in [12], we tackled the problem of security-aware multilayer planning with OTN encryption for packet-over-optical networks, by jointly considering the three architectures designed in [13].

FONs have been attracting R&D interests continuously since it was first proposed in [10]. Although they have obvious advantages in cost saving and energy efficiency, the broadcast-and-select nature of the optical communications in them also brings in a number of drawbacks, *e.g.*, inefficient spectrum utilization, more security vulnerabilities, and relatively complex network planning. Hence, people have studied how to improve the architecture of FONs to address these drawbacks. The work in [32, 33] investigated deploying FONs for metro networks with the horseshoe filterless architecture [34], which only contains two types of nodes, *i.e.*, the terminal nodes and the filterless nodes. Researchers also proposed the ideas of semi-filterless networks [35] and programmable filterless networks [36] to mitigate the drawbacks of FONs. Note that, with wavelength blockers (WBs), semi-filterless networks can better utilize spectrum resources [35], and this will be beneficial for the security-aware multilayer planning with OTN encryption. This is because WBs can avoid broadcasting optical signals to unexpected receivers [37, 38], and thus they can potentially reduce the numbers of used LCs/ECs/L-ECs.

One fundamental problem of the network planning of FONs is to design fiber trees to avoid laser-loops [18]. Previously, a few studies have considered the establishment of fiber trees for an FON and the resource allocation on them [39–45]. The study in [39] developed an algorithm to obtain the fiber tree establishment and RSA for the planning of an FON, and the authors also integrated the algorithm into a simulation tool based on MATLAB. Tremblay *et al.* [40] designed the fiber trees for an FON by leveraging the genetic algorithm and used tabu search to calculate the RSA in the fiber trees. Later, in [41], they still used the same method to establish fiber trees but proposed a heuristic algorithm to solve the RSA problem more time-efficiently. The survivable virtual network mapping problem was tackled in [42], where the authors proposed both an MILP model and heuristics. Jaumard *et al.* [43, 44] proposed novel one-step decomposition models for the optimal planning of FONs, which could solve the problems of fiber tree establishment and RSA simultaneously. In addition to the aforementioned studies on static planning of FONs, people have also considered dynamic service provisioning in FONs in [45]. Nevertheless, none of the studies mentioned above have addressed OTN encryption in FONs.

To the best our knowledge, our preliminary work in [16] is the only existing study that has addressed the security-aware multilayer planning of FONs with OTN encryption. This work greatly extends our study in [16] in a number of aspects, which justifies its novelty and contributions.

## III. Security-aware Multilayer Planning for FON with OTN Encryption

In this section, we first describe the problem of security-aware multilayer planning for an FON with OTN encryption, and then formulate an MILP to solve it exactly.

### A. Problem Description

We model the physical topology (*i.e.*, the fiber connections) to plan the FON as a graph $G(V, E)$, where $V$ and $E$ are the sets of nodes and directional links, respectively. Each node $v \in V$ is a filterless optical node that is built with passive splitters/combiners and the network elements in packet and encryption layers (*i.e.*, LCs, ECs, L-ECs, and an OTN switch). We set the capacity of each LC/EC/L-EC according to the values reported in [11, 13–15], *i.e.*, the set of feasible capacities of LCs/ECs/L-ECs is $B^c = \{40, 100, 400\}$ Gbps. The multilayer planning of the FON needs to serve a set of flows $\mathcal{R}$ from the packet layer, and we denote each flow as $r_i(s_i, d_i, b_i) \in \mathcal{R}$, where $i$ is its unique index, $s_i$/$d_i$ are its source/destination nodes, respectively, and $b_i$ is its bandwidth demand in Gbps.

We also assume that two nodes in $V$ can either have mutual trustiness or not. Therefore, for each flow, if its communication in the optical layer may be received by any node (except for its own destination) that does not have mutual trustiness with its source node, it should be encrypted with OTN encryption. The multilayer planning of the FON divides the physical topology into a few fiber trees [39], and the optical communications in each fiber tree use the broadcast-and-select scenario. If the source and destination nodes of a flow belong to different fiber trees, the flow has to be relayed in the packet or/and encryption layer at a common node of the two fiber trees.

Fig. 3 gives an illustrative example on the security-aware multilayer planning of an FON with OTN encryption. The table in Fig. 3(a) shows the information about the flows and the fiber trees and OTN encryption architectures used by them in Fig. 3(b). The subplot on the bottom right of Fig. 3(b) indicates the fiber trees in the optical layer, where the nodes that have mutual trustiness are marked with a same color, and the fiber links that belong to the same fiber tree are also colored the same. We establish four fiber trees for the FON, *i.e.*, *Trees* 1-4 covering *Nodes* $\{2, 3, 4\}$, $\{4, 6\}$, $\{1, 2, 3\}$ and $\{3, 4, 5, 6\}$, respectively. As shown in Fig. 3(a), there are 5 flows from the packet layer, and they are provisioned as follows.

Specifically, on *Node* 1, $r_1$ and $r_2$ are encrypted with two ECs, respectively, and then groomed by an LC, *i.e.*, leveraging the *Architecture* III in Fig. 1. $r_2$ is routed in *Trees* 3 and 4, in which multiple nodes (*Nodes* 2, 4, 5 and 6) are not trusted by its source (*Node* 1), and thus it is not decrypted until reaching its destination (*Node* 5). As for $r_3$, we allocate an L-EC on its source node (*Node* 2) to provision it with the *Architecture* IV in Fig. 1. As for $r_4$ and $r_5$, we first groom them to share

| $r(s,d)$ | Routed Fiber Trees | Architecture |
|---|---|---|
| $r_1(1,3)$ | Tree 3 | III |
| $r_2(1,5)$ | Trees 3 and 4 | I and III |
| $r_3(2,4)$ | Tree 1 | IV |
| $r_4(5,2)$ | Trees 1, 2 and 4 | I and II |
| $r_5(5,6)$ | Tree 4 | II |

(a)

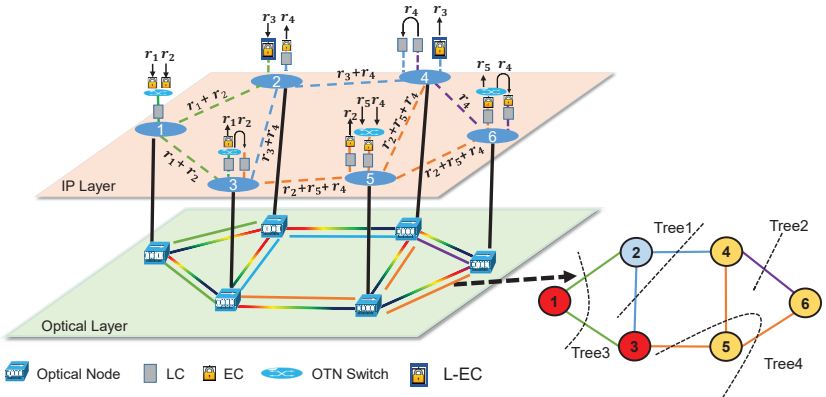


(b)

Fig. 3. Security-aware multilayer planning for an FON with OTN encryption.

the same bundle of LC and EC at their source node (*Node* 5) (*i.e.*, using the *Architecture* II in Fig. 1), then transmit the encrypted flows through a lightpath to the destination of $r_5$ (*Node* 6), where they are decrypted and de-groomed, next send the re-encrypted $r_4$ to *Node* 4 for going across two fiber trees (*i.e.*, using the *Architecture* I in Fig. 1), and finally forward the encrypted $r_4$ to its destination (*Node* 2) with *Tree* 1 (*i.e.*, still using the *Architecture* I in Fig. 1).

To this end, we can see that the security-aware multilayer planning tackled in this work needs to serve all the flows in $\mathcal{R}$ by establishing fiber trees to build an FON and jointly considering *Architectures* I-IV to allocate ECs/LCs/L-ECs in the FON, such that the total planning cost is minimized.

### *B. Optimization Model*

In the following, we formulate an MILP model to solve the optimization of the security-aware multilayer planning for an FON with OTN encryption, namely, the **w-MILP**. Note that, when formulating the optimization, we first determine the allocation of ECs and LCs, and then replace certain bundles of ECs and LCs with L-ECs if necessary.

**Parameters:**

- $G(V,E)$: the physical topology, where $V$ and $E$ are sets of nodes and fiber links, respectively.
- $L_{(u,v)}$: the length of a fiber link $(u,v) \in E$.
- $t_{u,v}$: the trustiness between two nodes $u$ and $v$, which equals 1 if node $u$ trusts node $v$, and 0 otherwise.
- $\mathcal{R}$: the set of flows from the packet layer, where the $i$-th flow in it is denoted as $r_i(s_i, d_i, b_i)$.
- $N$: the maximum number of LCs or ECs or L-ECs that can be allocated on a node[1], and the capacity of the $n$-th feasible LC/EC/L-EC on each node is preset as $b_n^c \in B^c$.
- $h_{\max}$: the maximum hop-count that a lightpath can be transmitted within a fiber tree before being received.
- $\alpha_n/\beta_n/\gamma_n$: the costs of the $n$-th feasible LC/EC/L-EC on a node, respectively.
- $M$: a big number.

[1]Here, although we do not explicitly consider the link bandwidth constraint, the available bandwidth on each link is actually bounded by the sum of the capacities of available LCs/ECs/L-ECs on the two end nodes of the link.

**Variables:**

- $Z^i_{(u,v)}$: the boolean variable that equals 1 if flow $r_i \in \mathcal{R}$ goes to the packet layer after link $(u,v)$, and 0 otherwise.
- $x^i_{n,v}$: the boolean variable that equals 1 if the $n$-th EC on node $v$ is allocated for flow $r_i$, and 0 otherwise.
- $y^i_{m,v}$: the boolean variable that equals 1 if the $m$-th LC on node $v$ is allocated for flow $r_i$, and 0 otherwise.
- $w^i_{m,n,v}$: the boolean variable that helps to determine the allocation of an L-EC, which equals 1 if the bundle of the $n$-th EC and the $m$-th LC allocated for $r_i$ on node $v$ can be replaced with an L-EC, and 0 otherwise.
- $N^{(1)}_{m,v}/N^{(2)}_{n,v}/N^{(3)}_{m,n,v}$: the auxiliary boolean variables that help to finalize the usage of an EC/LC/L-EC on node $v$.
- $C^{\text{LC}}_{m,v}$: the boolean variable that equals 1 if the $m$-th LC on node $v$ is used, and 0 otherwise.
- $C^{\text{EC}}_{n,v}$: the boolean variable that equals 1 if the $n$-th EC on node $v$ is used, and 0 otherwise.
- $C^{\text{L-EC}}_{k,v}$: the boolean variable that equals 1 if the $k$-th L-EC on node $v$ is used, and 0 otherwise.
- $X^{i,j}_{n,m,v}$: the boolean variable that equals 1 if the $n$-th and $m$-th ECs on node $v$ are allocated for flows $r_i$ and $r_j$, respectively, and 0 otherwise.
- $Y^{i,j}_{n,m,v}$: the boolean variable that equals 1 if the $n$-th and $m$-th LCs on node $v$ are allocated for flows $r_i$ and $r_j$, respectively, and 0 otherwise.
- $Q^i_{m,n,v}$: the boolean variable that equals 1 if the $m$-th LC and the $n$-th EC on node $v$ are allocated for flow $r_i$, and 0 otherwise.
- $P_{(u,v),k}$: the boolean variable that equals 1 if fiber links $(u,v)$ and $(v,u)$ are both in the $k$-th fiber tree ($k \in [1, \frac{|E|}{2}]$), and 0 otherwise[2].
- $F_{(u,v),k}$: the boolean variable that equals 1 if link $(u,v)$ is in the $k$-th fiber tree, and 0 otherwise.
- $T_{u,k}$: the boolean variable that equals 1 if node $u \in V$ is in the $k$-th fiber tree, and 0 otherwise.
- $o_k$: the boolean variable that equals 1 if the $k$-th fiber

[2]In this work, we consider directional fiber links in $E$, *i.e.*, $(u,v)$ and $(v,u)$ are two different links. Meanwhile, the working principle of FONs ensures that each pair of links between two nodes can only be included in one fiber tree [18]. Therefore, the maximum number of fiber trees that can be obtained in $G(V,E)$ is just half of the number of links in it (*i.e.*, $\frac{|E|}{2}$).

tree is designed, and 0 otherwise.

- $z_{v,k}$: the non-negative auxiliary integer variable that helps to avoid loops in the $k$-th fiber tree ($v \in V$).
- $\delta^i_{(u,v),k}$, $\varepsilon^i_{(u,v),k,p}$, $\zeta^{i,j}_{n,u}$, $\eta^{i,j}_{n,u}$, $\vartheta^i_{(u,v),(v,p),k}$, $\mu^i_{(u,v),(v,p),k}$, $\varpi^{i,j}_{(u,v)}$, $\rho^{i,j}_{(q,v)}$, $\phi^{i,j}_{(u,v),q}$, $\psi^{i,j}_{(u,v),q}$: the auxiliary boolean variables that are introduced for linearizing constraints.

**Objective:**

The optimization objective of the security-aware multilayer planning is to minimize the total cost of used LCs/ECs/L-ECs.

$$\begin{aligned}\text{Minimize}\quad 2\cdot\Bigg(&\sum_{v\in V}\sum_{m=1}^{N} C^{\text{LC}}_{m,v}\cdot\alpha_m+\sum_{v\in V}\sum_{n=1}^{N} C^{\text{EC}}_{n,v}\cdot\beta_n\\&+\sum_{v\in V}\sum_{k=1}^{N} C^{\text{L-EC}}_{k,v}\cdot\gamma_k\Bigg).\end{aligned}\tag{1}$$

**Constraints:**

*1) Constraints for Fiber Tree Establishment:*

$$\sum_{k\in[1,\frac{|E|}{2}]} P_{(u,v),k}=1,\quad \forall(u,v)\in E.\tag{2}$$

Eq. (2) ensures that the pair of directional links between nodes $u$ and $v$ must be included in one and only one fiber tree.

$$\begin{cases}\sum\limits_{(u,v)\in E} P_{(u,v),k}\le M\cdot T_{v,k},\\ \sum\limits_{(u,v)\in E} P_{(u,v),k}\ge T_{v,k},\end{cases}\quad \forall k\in[1,\frac{|E|}{2}],\ v\in V,\tag{3}$$

$$\sum_{(u,v)\in E} F_{(u,v),k}=\sum_{p\in V} T_{p,k}-o_k,\quad \forall k\in[1,\frac{|E|}{2}].\tag{4}$$

Eqs. (3) and (4) ensure that on a fiber tree, the relation between a pair of directional links and their end nodes is set correctly.

$$\begin{cases}\sum\limits_{(u,v)\in E} P_{(u,v),k}\ge o_k,\\ \sum\limits_{(u,v)\in E} P_{(u,v),k}\le o_k\cdot M,\end{cases}\quad \forall k\in[1,\frac{|E|}{2}],\ v\in V.\tag{5}$$

Eq. (5) ensures that the mapping between a pair of directional links and their fiber tree is determined correctly.

$$\begin{cases}P_{(u,v),k}=F_{(u,v),k}+F_{(v,u),k},\\ P_{(u,v),k}=P_{(v,u),k},\end{cases}\forall(u,v)\in E, k\in[1,\frac{|E|}{2}].\tag{6}$$

Eq. (6) ensures that on each fiber tree, the relation between a pair of directional links is determined correctly.

$$z_{u,k}-z_{v,k}+|V|\cdot F_{(u,v),k}\le|V|-o_k,\forall(u,v)\in E,k\in[1,\frac{|E|}{2}],\tag{7}$$

$$\sum_{(u,v)\in E} F_{(u,v),k}\le 1,\quad \forall k\in[1,\frac{|E|}{2}],\ v\in V.\tag{8}$$

Eqs. (7) and (8) ensure that there is no loop in each fiber tree.

*2) Constraints for Flow Routing:*

$$\sum_{(u,v)\in E} Z^i_{(u,v)}-\sum_{(v,u)\in E} Z^i_{(v,u)}=\begin{cases}1, & u=s_i,\\ -1, & u=d_i,\\ 0, & \text{otherwise},\end{cases}\quad \forall r_i\in\mathcal{R},\ u\in V.\tag{9}$$

Eq. (9) is the flow conservation condition that ensures a flow $r_i \in R$ being routed in a single path from source to destination. On the left side of Eq. (9), the first/second terms denote the total numbers of outgoing/incoming links used by $r_i$, respectively. Note that, Eq. (9) cannot prevent routing loops, but as routing loops usually require more LCs/ECs/L-ECs, they will normally be ruled out by the optimization objective.

$$h_{\max}\ge\sum_{(u,v)\in E} P_{(u,v),k}\cdot Z^i_{(u,v)},\quad \forall k\in[1,\frac{|E|}{2}],\ r_i\in\mathcal{R}.\tag{10}$$

Eq. (10) limits the maximum hop that each flow can be transmitted in a fiber tree before being received.

$$\begin{cases}\delta^i_{(u,v),k}\le Z^i_{(u,v)},\\ \delta^i_{(u,v),k}\le P_{(u,v),k},\\ \delta^i_{(u,v),k}\ge P_{(u,v),k}+Z^i_{(u,v)}-1,\end{cases}\quad \forall r_i,\ (u,v),\ k,\tag{11}$$

$$h_{\max}\ge\sum_{(u,v)\in E}\delta^i_{(u,v),k},\quad \forall k,\ r_i.\tag{12}$$

As Eq. (10) is nonlinear, Eqs. (11) and (12) linearize it.

*3) Constraints for Allocating LCs:*

$$\sum_{r_i\in\mathcal{R}} y^i_{m,v}\cdot b_i\le b^c_m,\quad \forall m\in[1,N],\ v\in V.\tag{13}$$

Eq. (13) ensures that the total bandwidth demand of the flows using a same LC does not exceed the capacity of the LC.

$$\begin{aligned}\sum_{n\in[1,N]} y^i_{n,v}\ge Z^i_{(u,v)}\cdot Z^i_{(v,p)}\cdot P_{(u,v),k}\cdot\left[1-P_{(v,p),k}\right],\\ \forall r_i\in\mathcal{R},\ \forall(u,v),(v,p)\in E,\ \forall k\in[1,\frac{|E|}{2}].\end{aligned}\tag{14}$$

Eq. (14) ensures that LCs are allocated to bridge flows for going across fiber trees.

$$\begin{cases}\vartheta^i_{(u,v),(v,p),k}\le Z^i_{(v,p)},\\ \vartheta^i_{(u,v),(v,p),k}\le\delta^i_{(u,v),k},\\ \vartheta^i_{(u,v),(v,p),k}\ge Z^i_{(v,p)}+\delta^i_{(u,v),k}-1,\end{cases}\quad \forall(u,v),(v,p)\in E,\ \forall r_i\in\mathcal{R},\ \forall k\in[1,\frac{|E|}{2}],\tag{15}$$

$$\begin{cases}\mu^i_{(u,v),(v,p),k}\le P_{(v,p),k},\\ \mu^i_{(u,v),(v,p),k}\le\vartheta^i_{(u,v),(v,p),k},\\ \mu^i_{(u,v),(v,p),k}\ge P_{(v,p),k}+\vartheta^i_{(u,v),(v,p),k}-1,\end{cases}\quad \forall(u,v),(v,p)\in E,\ \forall r_i\in\mathcal{R},\ \forall k\in[1,\frac{|E|}{2}],\tag{16}$$

$$\begin{aligned}\sum_{n\in[1,N]} y^i_{n,v}\ge\vartheta^i_{(u,v),(v,p),k}-\mu^i_{(u,v),(v,p),k},\\ \forall(u,v),(v,p)\in E,\ \forall r_i\in\mathcal{R},\ \forall k\in[1,\frac{|E|}{2}].\end{aligned}\tag{17}$$

As Eq. (14) is nonlinear, Eqs. (15)-(17) linearize it.

$$\sum_{n=1}^{N} y^i_{n,s_i}=1,\quad \forall r_i\in\mathcal{R}.\tag{18}$$

Eq. (18) ensures that an LC must be allocated for each flow on its source node.

$$\begin{cases}Y^{i,j}_{n,m,v}\le y^i_{n,v},\\ Y^{i,j}_{n,m,v}\le y^j_{m,v},\\ Y^{i,j}_{n,m,v}\ge y^i_{n,v}+y^j_{m,v}-1,\end{cases}\quad \forall n,m\in[1,N],\ v\in V,\ r_i,r_j\in\mathcal{R},\tag{19}$$

$$\sum_{(d_i,v)\in E} Z^j_{(d_i,v)}\cdot Y^{i,j}_{n,n,u}\le\sum_{n'\in[1,N]} y^j_{n',d_i},\quad \forall r_i,r_j\in\mathcal{R},\ n\in[1,N],\ u\in V.\tag{20}$$

Eqs. (19) and (20) ensure that if a flow is de-groomed from other flows by an LC on a node other than its destination, the flow must be re-groomed by an LC on that node.

$$\begin{cases} \eta^{i,j}_{n,u} \le \sum\limits_{(d_i,v)\in E} Z^j_{(d_i,v)}, \\ \eta^{i,j}_{n,u} \le Y^{i,j}_{n,n,u}, \\ \eta^{i,j}_{n,u} \ge Y^{i,j}_{n,n,u} + \sum\limits_{(d_i,v)\in E} Z^j_{(d_i,v)} - 1, \end{cases} \quad \forall r_i, r_j \in \mathcal{R},\ u,\ n, \tag{21}$$

$$\eta^{i,j}_{n,u} \le \sum_{n'\in[1,N]} y^j_{n',d_i},\ \forall r_i, r_j \in \mathcal{R}, n, u. \tag{22}$$

As Eq. (20) is nonlinear, Eqs. (21) and (22) linearize it.

$$\begin{cases} \varpi^{i,j}_{(u,v)} \le Z^i_{(u,v)}, \\ \varpi^{i,j}_{(u,v)} \le Z^j_{(u,v)}, \\ \varpi^{i,j}_{(u,v)} \ge Z^i_{(u,v)} + Z^j_{(u,v)} - 1, \end{cases} \quad \forall r_i, r_j \in \mathcal{R},\ (u,v) \in E, \tag{23}$$

$$\begin{cases} \rho^{i,j}_{(q,v)} \le \varpi^{i,j}_{(q,v)}, \\ \rho^{i,j}_{(q,v)} \le 1 - \sum\limits_{(v,p)\in E} \varpi^{i,j}_{(v,p)}, \\ \rho^{i,j}_{(q,v)} \ge \varpi^{i,j}_{(q,v)} + \sum\limits_{(v,p)\in E} \varpi^{i,j}_{(v,p)}, \end{cases} \quad \forall r_i, r_j \in \mathcal{R},\ \{(q,v) : (q,v) \in E,\ v \ne d_i, d_j\}. \tag{24}$$

Eqs. (23) and (24) mark the nodes where the flows sharing one LC are de-groomed.

$$\sum_{(u,v)\in E} \varpi^{i,j}_{(u,v)} \ge \sum_{m\in[1,N]} Y^{i,j}_{m,m,u},\ \forall u \in V,\ \forall r_i, r_j \in \mathcal{R}, \tag{25}$$

$$\begin{aligned} &\sum_{n\in[1,N]} Y^{i,j}_{n,n,u} \cdot \left(Z^j_{(q,v)} \cdot Z^i_{(q,v)}\right) \cdot \left(1 - \sum_{(v,p)\in E} Z^j_{(v,p)} \cdot Z^i_{(v,p)}\right) \\ &\le \sum_{n,n'\in[1,N],n\ne n'} Y^{i,j}_{n,n',v}, \quad \forall (q,v) \in E,\ r_i, r_j \in \mathcal{R}, \\ &\forall u \in V,\ \{v : v \in V, v \ne u, d_i, d_j\}. \end{aligned} \tag{26}$$

Eqs. (25) and (26) ensure that if flows groomed by one LC are de-groomed by an LC on a node other than their destinations, LCs must be allocated on the node to re-groom them.

$$\begin{cases} \phi^{i,j}_{(q,v),u} \le \sum\limits_{n\in[1,N]} Y^{i,j}_{n,n,u}, \\ \phi^{i,j}_{(q,v),u} \le \rho^{i,j}_{(q,v)}, \\ \phi^{i,j}_{(q,v),u} \ge \rho^{i,j}_{(q,v)} + \sum\limits_{n\in[1,N]} Y^{i,j}_{n,n,u} - 1, \end{cases} \quad \forall (q,v) \in E, r_i, r_j \in \mathcal{R}, u \in V, \{v : v \in V, v \ne u, d_i, d_j\}, \tag{27}$$

$$\sum_{n,m\in[1,N],n\ne m} Y^{i,j}_{n,m,v} \ge \phi^{i,j}_{(q,v),u}, \quad \forall (q,v) \in E, r_i, r_j \in \mathcal{R}, u \in V, \{v : v \in V, v \ne u, d_i, d_j\}. \tag{28}$$

As Eq. (26) is nonlinear, Eqs. (27) and (28) linearize it.

*4) Constraints for Allocating ECs:*

$$\sum_{r_i\in\mathcal{R}} x^i_{n,v} \cdot b_i \le b^c_n, \quad \forall n \in [1,N],\ v \in V. \tag{29}$$

Eq. (29) ensures that the total bandwidth demand of the flows using a same EC does not exceed the capacity of the EC.

$$\sum_{n\in[1,N]} x^i_{n,s_i} \ge Z^i_{(u,v)} \cdot P_{(u,v),k} \cdot T_{p,k} \cdot (1 - t_{s_i,p}), \quad \forall r_i \in \mathcal{R},\ (u,v) \in E,\ k \in [1, \frac{|E|}{2}],\ \{p : p \in V, p \ne d_i\}. \tag{30}$$

Eq. (30) ensures that for each flow $r_i \in \mathcal{R}$, if any node (except for its destination $d_i$) in a fiber tree carrying it is not trusted by its source $s_i$, the flow must be encrypted at $s_i$.

$$\begin{cases} \varepsilon^i_{(u,v),k,p} \le \delta^i_{(u,v),k}, \\ \varepsilon^i_{(u,v),k,p} \le T_{p,k}, \\ \varepsilon^i_{(u,v),k,p} \ge \delta^i_{(u,v),k} + T_{p,k} - 1, \end{cases} \quad \forall r_i \in \mathcal{R},\ (u,v) \in E,\ p \in V,\ k \in [1, \frac{|E|}{2}], \tag{31}$$

$$\sum_{n\in[1,N]} x^i_{n,s_i} \ge \varepsilon^i_{(u,v),k,p} \cdot (1 - t_{s_i,p}), \quad \forall r_i \in \mathcal{R},\ (u,v) \in E,\ k \in [1, \frac{|E|}{2}],\ \{p : p \in V, p \ne d_i\}. \tag{32}$$

As Eq. (30) is nonlinear, Eqs. (31) and (32) linearize it.

$$\sum_{n\in[1,N]} x^i_{n,v} \le t_{s_i,v}, \quad \forall r_i \in \mathcal{R},\ v \in V. \tag{33}$$

Eq. (33) ensures that a flow cannot be decrypted on the nodes, which are not trusted by its source (except for its destination).

$$\begin{cases} X^{i,j}_{n,m,v} \le x^i_{n,v}, \\ X^{i,j}_{n,m,v} \le x^j_{m,v}, \\ X^{i,j}_{n,m,v} \ge x^i_{n,v} + x^j_{m,v} - 1, \end{cases} \quad \forall n, m \in [1,N], r_i, r_j \in \mathcal{R}, v \in V, \tag{34}$$

$$\sum_{(d_i,v)\in E} Z^j_{(d_i,v)} \cdot X^{i,j}_{n',n',u} \le \sum_{n\in[1,N]} x^j_{n,d_i}, \quad \forall r_i, r_j \in \mathcal{R},\ n' \in [1,N],\ u \in V. \tag{35}$$

Eq. (34) and (35) ensure that if a flow is decrypted with other flows by an EC on a node other than its destination, the flow must be re-encrypted by an EC on that node.

$$\begin{cases} \zeta^{i,j}_{n,u} \le \sum\limits_{(d_i,v)\in E} Z^j_{(d_i,v)}, \\ \zeta^{i,j}_{n,u} \le X^{i,j}_{n,n,u}, \\ \zeta^{i,j}_{n,u} \ge X^{i,j}_{n,n,u} + \sum\limits_{(d_i,v)\in E} Z^j_{(d_i,v)} - 1, \end{cases} \quad \forall r_i, r_j \in \mathcal{R},\ (u,v) \in E,\ k \in [1, \frac{|E|}{2}], \tag{36}$$

$$\zeta^{i,j}_{n',u} \le \sum_{n\in[1,N]} x^j_{n,d_i},\ \forall r_i, r_j \in \mathcal{R}, n' \in [1,N], u \in V. \tag{37}$$

As Eq. (35) is nonlinear, Eqs. (36) and (37) linearize it.

$$\begin{aligned} &\sum_{n\in[1,N]} X^{i,j}_{n,n,u} \cdot (Z^j_{q,v} \cdot Z^i_{q,v}) \cdot \left(1 - \sum_{(v,p)\in E} Z^j_{v,p} \cdot Z^i_{v,p}\right) \\ &\le \sum_{n,n'\in[1,N],n\ne n'} X^{i,j}_{n,n',v},\ \forall r_i, r_j \in \mathcal{R}, u \in V, \\ &\{(q,v) : (q,v) \in E, v \ne u, d_i, d_j\}, \end{aligned} \tag{38}$$

Eq. (38) ensures that if flows share one EC are decrypted by an EC on a node other than their destinations, ECs must be allocated on the node to re-encrypted them.

$$\begin{cases} \psi^{i,j}_{(q,v),u} \le \sum\limits_{n\in[1,N]} X^{i,j}_{n,n,u}, \\ \psi^{i,j}_{(q,v),u} \le \rho^{i,j}_{(q,v)}, \\ \psi^{i,j}_{(q,v),u} \ge \rho^{i,j}_{(q,v)} + \sum\limits_{n\in[1,N]} X^{i,j}_{n,n,u} - 1, \end{cases} \quad \forall r_i, r_j \in \mathcal{R},\ u \in V,\ \{(q,v) : (q,v) \in E, v \ne u, d_i, d_j\}, \tag{39}$$

$$\sum_{n,m\in[1,N],n\ne m} X^{i,j}_{n,m,v} \ge \psi^{i,j}_{(q,v),u}, \quad \forall r_i, r_j \in \mathcal{R},\ u \in V,\ \{(q,v) : (q,v) \in E, v \ne u, d_i, d_j\}. \tag{40}$$

As Eq. (38) is nonlinear, Eqs. (39) and (40) linearize it.

*5) Constraints for Mapping Flows to LCs and ECs:*

$$\sum_{n=1}^{N} X_{n,n,v}^{i,j} \leq \sum_{m=1}^{N} Y_{m,m,v}^{i,j} \leq 1, \quad \forall r_i, r_j \in \mathcal{R},\ v \in V. \tag{41}$$

Eq. (41) ensures that each flow has to use an LC, and the flows sharing an EC have to use the LC connecting to the EC.

$$\begin{cases} Q_{m,n,v}^{i} \leq y_{m,v}^{i}, \\ Q_{m,n,v}^{i} \leq x_{n,v}^{j} \leq 1, \\ Q_{m,n,v}^{i} \geq y_{m,v}^{i} + x_{n,v}^{j} - 1, \end{cases} \quad \forall n, m \in [1, N],\ v,\ r_i, \tag{42}$$

$$b_m^c \geq \sum_{n \in [1,N]} \sum_{r_i \in \mathcal{R}} Q_{n,m,v}^{i} \cdot b_n^c, \quad \forall v \in V,\ m \in [1, N]. \tag{43}$$

Eq. (42) and (43) ensure that the total capacity of the ECs, which connect to an LC, does not exceed the LC's capacity.

*6) Constraints for Allocating L-ECs:*

$$\begin{aligned} M \cdot (1 - w_{n',m',u}^{i}) \geq & \sum_{r_j \in \mathcal{R}, v \in V} \left( \sum_{m=1}^{N} Y_{m,v}^{i,j} - \sum_{n=1}^{N} X_{n,v}^{i,j} \right) \\ & + (1 - Q_{m',n',u}) + |b_{m'}^c - b_{n'}^c|,\ \forall n', m' \in [1, N], u, r_i. \end{aligned} \tag{44}$$

Eq. (44) ensures that L-ECs replace LCs and ECs properly.

*7) Constraints for Numbers of LCs, ECs and L-ECs:*

$$\begin{cases} N_{n,v}^{(2)} \leq \sum_{r_i \in R} x_{n,v}^{i}, \\ \sum_{r_i \in R} x_{n,v}^{i} \leq M \cdot N_{n,v}^{(2)}, \end{cases} \quad \forall v \in V,\ n \in [1, N]. \tag{45}$$

Eq. (45) gets the number of ECs allocated on each node.

$$\begin{cases} N_{n,v}^{(1)} \leq \sum_{r_i \in \mathcal{R}} y_{n,v}^{i}, \\ \sum_{r_i \in \mathcal{R}} y_{n,v}^{i} \leq M \cdot N_{n,v}^{(1)}, \end{cases} \quad \forall v \in V,\ n \in [1, N]. \tag{46}$$

Eq. (46) gets the number of LCs allocated on each node.

$$\begin{cases} N_{m,n,v}^{(3)} \leq \sum_{r_i \in \mathcal{R}} w_{m,n,v}^{i}, \\ \sum_{r_i \in \mathcal{R}} w_{m,n,v}^{i} \leq M \cdot N_{m,n,v}^{(3)} \end{cases} \quad \forall v \in V,\ m, n \in [1, N]. \tag{47}$$

Eq. (47) gets the number of L-ECs allocated on each node.

$$\begin{cases} C_{m,v}^{\text{LC}} = N_{m,v}^{(1)} - \sum_{n=1}^{N} N_{m,n,v}^{(3)}, \\ C_{n,v}^{\text{EC}} = N_{n,v}^{(2)} - \sum_{m=1}^{N} N_{m,n,v}^{(3)}, \\ C_{n,v}^{\text{L-EC}} = \sum_{m=1}^{N} N_{m,n,v}^{(3)}, \end{cases} \quad \forall m \in [1, N],\ v \in V. \tag{48}$$

Eq. (48) gets the allocations of ECs/LCs/L-ECs on each node.

**Theorem 1.** *The security-aware multilayer planning of FON described by the aforementioned MILP model is $\mathcal{NP}$-hard.*

*Proof:* We prove that the optimization is $\mathcal{NP}$-hard by the restriction method [46], *i.e.*, reducing it to a special case that is the general case of a known $\mathcal{NP}$-hard problem. Specifically, we apply the following restrictions:

- We set $\beta_n = \gamma_n = 0$, *i.e.*, ECs and L-ECs are free when counting the total cost.
- We set $h_{\max} = +\infty$, *i.e.*, the constraint on the maximum hop that a lightpath can be transmitted within a fiber tree before being received is relaxed.
- We assume that the physical topology only contains two nodes and two directional links between them, *i.e.*, one fiber tree can be set up for the FON.
- We set $|B^c| = 1$, *i.e.*, the number of feasible LC capacities is 1 (all the LCs have the same capacity).

Then, the security-aware multilayer planning is transformed to the problem where a set of flows should be groomed onto the least number of fixed-capacity LCs. This problem is equivalent to the general case of bin packing [46], if we treat the flows as items and the LCs as bins. As bin packing is an $\mathcal{NP}$-hard problem, the optimization in w-MILP is also $\mathcal{NP}$-hard. ■

## IV. Algorithm Design

Since the optimization formulated in the previous section is $\mathcal{NP}$-hard, it can become intractable for large-scale problems. Therefore, we design time-efficient algorithms for it in this section. Note that, due to the complexity of w-MILP (*i.e.*, it contains large numbers of variables and constraints), we have difficulty designing an approximation algorithm for it directly. Meanwhile, it is a common practice to reduce the time complexity of FON planning by considering pre-calculated fiber trees [41, 47]. Therefore, we divide the original optimization into two subproblems: 1) the establishment of fiber trees with pre-calculated ones, and 2) the allocation of LCs/ECs/L-ECs based on the selected fiber trees, and solve them sequentially[3]. Polynomial-time approximation algorithms will be designed for the two subproblems in the following.

### A. Establishment of Fiber Trees

For establishing the fiber trees for an FON, we first precalculate a set of tree-type subgraphs in $G(V, E)$ and store them in set $\mathcal{F}$. Specifically, each tree-type subgraph (*i.e.*, each fiber tree) covers $n$ nodes ($n \in [2, |V| - 1]$), which are randomly selected from $V$. Note that, the number of pre-calculated fiber trees in $\mathcal{F}$ is not fixed, and it is set empirically[4]. We assign a weight $c_{tr}$ to each tree $tr \in \mathcal{F}$, based on the potential cost of LCs/ECs that might be generated if the tree is selected as a fiber tree of the FON. The weight is

$$c_{tr} = 1 + \lambda \cdot \sum_{r_i \in \mathcal{R}} \chi_{i,tr}, \quad \forall tr \in \mathcal{F}, \tag{49}$$

where $\lambda$ is the average cost ratio between ECs and LCs, $\chi_{i,tr}$ is a boolean indicator that equals 1 if flow $r_i$ has to be encrypted in fiber tree $tr$, and 0 otherwise. Hence, the weight considers not only the costs of LCs/ECs but also the trustiness between

[3]This scheme might not solve the original optimization exactly. Specifically, compared with w-MILP, a performance gap will be generated due to two factors: 1) the first subproblem is formulated based on a set of pre-calculated fiber trees, which might not explore the whole solution space, and 2) solving the two subproblems sequentially only examines a part of the whole solution space. However, because of the complexity of w-MILP, it is difficult for us to analyze the performance gap theoretically. The gap can be evaluated with simulations for small-scale problems, while for large-scale problems, it can be reduced by inputting more pre-calculated fiber trees to the first subproblem.

[4]Generally speaking, we will include more fiber trees in $\mathcal{F}$ if the FON topology $G(V, E)$ is larger or/and $\mathcal{R}$ contains more flows, and *vice versa*.

node pairs. Then, the fiber tree establishment is to select proper trees from $\mathcal{F}$ to cover all the links in $G(V,E)$, such that the total weight of the selected trees is minimized.

**Variables:**

- $\pi_{tr}$: the boolean variable that equals 1 if a tree $tr \in \mathcal{F}$ is selected as a fiber tree for the FON, and 0 otherwise.

**Parameters:**

- $\mathcal{F}$: the set of precalculated trees in $G(V,E)$.
- $c_{tr}$: the cost of a tree $tr \in \mathcal{F}$.
- $a_{e,tr}$: the boolean parameter that equals 1 if link $e \in E$ is included in tree $tr$, and 0 otherwise.

**Objective:**

$$\text{Minimize} \quad \sum_{tr\in\mathcal{F}} c_{tr}\cdot\pi_{tr}. \tag{50}$$

**Constraints:**

$$\sum_{tr\in\mathcal{F}} \pi_{tr}\cdot a_{e,tr} = 1, \quad \forall e \in E. \tag{51}$$

Eq. (51) ensures that each link in the physical topology is included in one and only one fiber tree of the FON.

The optimization above (*i.e.*, **t-MILP**) is equivalent to the problem of weighted set partitioning [48]. Although it is still an $\mathcal{NP}$-hard problem, its formulation is compact and thus it can be solved quickly if the physical topology $G(V,E)$ is not very large. Meanwhile, there are a few existing approximation algorithms that can solve large-scale weighted set partitioning problems time-efficiently [48]. Therefore, we do not need to design an approximation algorithm for it here.

### *B. Allocation of LCs/ECs/L-ECs*

After determining fiber trees for the FON, we only need to keep Eqs. (9)-(48) to formulate the subproblem for allocating LCs/ECs/L-ECs. By leveraging the proof of $\mathcal{NP}$-hardness in Section III-B, we can easily verify that the subproblem for allocating LCs/ECs/L-ECs is still $\mathcal{NP}$-hard. Therefore, we propose a polynomial-time approximation algorithm to solve it based on linear programming (LP) relaxation and randomized rounding [49], which can obtain near-optimal solutions whose performance gap to the optimal ones is bounded.

First of all, we notice that after relaxing the MILP with Eqs. (9)-(48) to an LP and solving it, certain variables might not satisfy the original constraints and produce an infeasible solution. To address this issue, we change Eq. (9) to

$$\begin{cases} \sum\limits_{(s_i,v)\in E} Z^i_{(s_i,v)} = \sum\limits_{(v,d_i)\in E} Z^i_{(v,d_i)} = 1, \ \forall r_i \in \mathcal{R}, \\ \sum\limits_{(v,s_i)\in E} Z^i_{(v,s_i)} = \sum\limits_{(d_i,v)\in E} Z^i_{(v,d_i)} = 0, \ \forall r_i \in \mathcal{R}, \\ \sum\limits_{(u,v)\in E} Z^i_{(u,v)} - \sum\limits_{(v,u)\in E} Z^i_{(v,u)} = 0, \ \forall r_i, \{u : u \neq s_i, d_i\}. \end{cases} \tag{52}$$

We also introduce coefficients $\{\zeta_1 \in (0,1)\}$ to tighten the capacities of feasible LCs/ECs/L-ECs on each node as

$$b^{c*}_n = b^c_n \cdot \zeta_1, \quad \forall n \in [1,N], \tag{53}$$

and replace the corresponding $\{b^c_n\}$ in Eqs. (13), (29) and (43) with $\{b^{c*}_n\}$ in Eq. (53). Note that, tightening the capacity constraints might not eliminate the possibility of infeasible solutions, and thus we also use other methods in our proposed approximation algorithm (*Algorithm* 1) to address it.

The subproblem for allocating of LCs/ECs/L-ECs is formulated as follows, which will be referred to as **s-MILP** in the rest of the paper. Eqs. (13), (29) and (43) are tightened ones when solving relaxed s-MILP.

$$\text{Minimize} \quad \mathcal{C} = 2\cdot\sum_{v\in V}\left(\sum_{m=1}^{N} C^{\text{LC}}_{m,v}\cdot\alpha_m + \sum_{n=1}^{N} C^{\text{EC}}_{n,v}\cdot\beta_n + \sum_{k=1}^{N} C^{\text{L-EC}}_{k,v}\cdot\gamma_k\right)$$
$$\text{s.t.} \quad \text{Eqs. (9)-(48), and (52).} \tag{54}$$

**Algorithm 1:** Approximation Algorithm to Solve s-MILP

**Input**: Parameters of s-MILP, $\{P_{(u,v),k}, T_{v,k}\}$ about fiber trees, $Q_1$ and $Q_2$, $\mathcal{C} = +\infty$.
**Output**: Allocation of LCs/ECs/L-ECs, total cost $\mathcal{C}$.

relax s-MILP in Eq. (54) to get an LP;
solve the LP to get values of $\{Z^i_{(u,v)}\}$ in real numbers;
put the obtained $\{Z^i_{(u,v)}\}$ in s-MILP as parameters to transform it to a more compact model, and relax the compact model to get a new LP;
solve the new LP to get values of $\{y^i_{m,v}, x^i_{n,v}\}$ and its objective $\mathcal{C}_{\text{LP}}$ in real numbers;
**for** $q_1 = 1$ *to* $Q_1$ **do**
  **for** *each flow* $r_i \in \mathcal{R}$ **do**
    $p = s_i$, $\mathcal{P}_i = \emptyset$;
    **while** $p \neq d_i$ **do**
      $\delta_1 = 1 - \sum\limits_{(p,v)\in E} Z^i_{(p,v)}$, and distribute the value of $\delta_1$ evenly to each non-zero $Z^i_{(p,v)}$;
      randomly select a link $(p,v)$ to set $Z^i_{(p,v)} = 1$ with probabilities of $\{Z^i_{(p,v)}\}$;
      update $\{Z^i_{(p,v)}\}$ accordingly, insert $(p,v)$ into path $\mathcal{P}_i$, and set $p = v$;
    **end**
    obtain the nodes that have to use LCs or ECs according to $\{\mathcal{P}_i, T_{u,k}, t_{u,v}\}$, and store them into sets $V^{\text{LC}}_i$ and $V^{\text{EC}}_i$, respectively;
    **for** $v \in V^{LC}_i$ **do**
      $\delta_2 = 1 - \sum\limits_{m\in[1,N]} y^i_{m,v}$, and distribute the value of $\delta_2$ evenly to each non-zero $y^i_{m,v}$;
    **end**
    **for** $v \in V^{EC}_i$ **do**
      $\delta_3 = 1 - \sum\limits_{n\in[1,N]} x^i_{n,v}$, and distribute the value of $\delta_3$ evenly to each non-zero $x^i_{n,v}$;
    **end**
  **end**
  invoke *Algorithm* 2 to get the current optimal cost $\hat{\mathcal{C}}$;
  $\mathcal{C} = \min(\mathcal{C}, \hat{\mathcal{C}})$;
**end**

The procedure of our proposed polynomial-time approximation algorithm to solve the subproblem is shown in *Algorithms* 1 and 2, where *Algorithm* 2 is a sub-procedure of *Algorithm* 1. In addition to the information about the fiber trees, flows and feasible LCs/ECs/L-ECs, the algorithms also take two positive

**Algorithm 2:** Sub-procedure of Approximation Algorithm

**Input**: inputs of *Algorithm* 1, $\{V_i^{\text{LC}}, V_i^{\text{EC}}, \mathcal{P}_i\}$, $\hat{\mathcal{C}} = +\infty$.
**Output**: $\hat{\mathcal{C}}$.

1 **for** $q_2 = 1$ *to* $Q_2$ **do**
2  **for** *each node* $v \in V$ **do**
3  randomly select $m$-th LC or $n$-th EC to set $y_{m,v}^i = 1$ or $x_{n,v}^i = 1$ with probabilities of $\{y_{m,v}^i\}$ or $\{x_{n,v}^i\}$, respectively;
4  **end**
5  **for** *each node* $v \in V$ **do**
6  $\mathcal{R}' = \mathcal{R}_1 = \mathcal{R}_1' = \mathcal{R}_2 = \mathcal{R}_2' = \mathcal{R}_3 = \emptyset$;
7  **for** $m \in [1, N]$ **do**
8  find the flows with $y_{m,v}^i > 0$, and sort them in descending order of $\{y_{m,v}^i\}$ to store in set $\mathcal{R}'$;
9  insert the first flow $r_1' \in \mathcal{R}'$ into $\mathcal{R}_1'$ and $\mathcal{R}_2'$;
10  **for** $j = 2$ *to* $|\mathcal{R}'|$ **do**
11  **if** $r_j'$ *and* $r_1'$ *can share* $m$*-th LC on* $v$ **then**
12  insert $r_j'$ into $\mathcal{R}_1'$;
13  **if** *the source of* $r_j'$ *trusts* $v$ **then**
14  insert $r_j'$ into $\mathcal{R}_2'$;
15  **end**
16  **else**
17  insert $r_j'$ into $\mathcal{R}_1$;
18  **end**
19  **end**
20  reallocate an available and most suitable LC to each flow in $\mathcal{R}_1'$ and $\mathcal{R}_1$;
21  **for** $n \in [1, N]$ **do**
22  find the flows in $\mathcal{R}_2'$ that can share $n$-th EC on $v$, and insert them into $\mathcal{R}_3$;
23  insert the remaining flows in $\mathcal{R}_2'$ into $\mathcal{R}_2$;
24  **end**
25  reallocate an available and most suitable EC to each flow in $\mathcal{R}_3$ and $\mathcal{R}_2$;
26  **end**
27  **end**
28  finalize the allocation of LCs and ECs;
29  replace bundles of LCs/ECs with L-ECs if proper;
30  calculate the total cost $\mathcal{C}$ with Eq. (54);
31  $\hat{\mathcal{C}} = \min(\mathcal{C}, \hat{\mathcal{C}})$;
32 **end**

integers (*i.e.*, $Q_1$ and $Q_2$) as their inputs, which are introduced to adjust the tradeoff between the time complexity and performance of our approximation algorithm. We determine the values of $Q_1$ and $Q_2$ empirically, according to the way in [50].

In *Algorithm* 1, we first relax s-MILP to get an LP (*Line* 1). Note that, the relaxation can make some variables not satisfy the original constraints and thus generate infeasible solutions. For example, the constraint in Eq. (14) cannot be guaranteed after the relaxation, which will lead to infeasible solutions of $\{y_{m,v}^i\}$. Therefore, we introduce the technique in *Lines* 2 and 3 to leverage the solutions of $\{Z_{(u,v)}^i\}$ to obtain a new LP. Then, the infeasible solutions of $\{y_{m,v}^i\}$ caused by the relaxation can be avoided, and we solve the new LP to get decision variables $\{y_{m,v}^i, x_{n,v}^i\}$ and the objective $\mathcal{C}_{\text{LP}}$ in *Line* 4.

*Lines* 5-23 show the overall procedure of randomized rounding. Each iteration of the randomized rounding checks each flow $r_i \in \mathcal{R}$ to serve it with LCs/ECs/L-ECs. We first find a feasible routing path for $r_i$ with *Lines* 7-12. Then, we obtain the nodes on which $r_i$ needs to use LCs or ECs in *Line* 13. Next, the for-loops covering *Lines* 14-16 and *Lines* 17-19 ensure that if an LC or an EC needs to be allocated for $r_i$ on a node, the total of the corresponding probabilities (*i.e.*, the values of decision variables $\{y_{m,v}^i\}$ or $\{x_{n,v}^i\}$) is 1, respectively. *Line* 21 invokes *Algorithm* 2 to get the allocation of LCs/ECs/L-ECs and the current total cost $\hat{\mathcal{C}}$. Finally, *Lines* 22 updates the minimum cost that has been found so far.

*Algorithm* 2 explains how to leverage randomized rounding to build a feasible solution for the allocation of LCs/ECs/L-ECs, which still operates in iterations. *Lines* 2-4 randomly choose an LC/EC to serve flow $r_i$ on a node $v$ if necessary. Then, the for-loop of *Lines* 5-27 determines the preliminary allocation of LCs/ECs for each flow. Specifically, *Lines* 8-20 check whether flows can share LCs on a node $v$ and allocate the most suitable LC for each flow, where *Lines* 13-15 store the flows that may share ECs on node $v$ in set $\mathcal{R}_2'$. *Lines* 21-25 check whether flows can share ECs on a node $v$ and allocate the most suitable EC for each flow. *Line* 28 finalizes the allocation of LCs/ECs by consolidating to remove redundant LCs/ECs. Next, we replace bundles of LCs/ECs with L-ECs in *Line* 29. Finally, in *Lines* 30-31, we calculate the total cost $\mathcal{C}$, and update the current optimal cost $\hat{\mathcal{C}}$ if necessary.

### C. Theoretical Analysis of Proposed Algorithms

**Theorem 2.** *The randomized rounding in* Algorithm *1 can converge to ensure a bounded approximation ratio.*

*Proof:* We denote the optimal cost from s-MILP as $\mathcal{C}_{\text{s-MILP}}$ and introduce a coefficient $\varepsilon \geq 1$. Then, we define the probability that *Algorithm* 1 obtains a solution whose cost is not less than $\varepsilon \cdot \mathcal{C}_{\text{s-MILP}}$ in each iteration as $\mathbf{P} = \mathbb{P}(\hat{\mathcal{C}} \geq \varepsilon \cdot \mathcal{C}_{\text{s-MILP}})$. According to [50], we have $\mathbf{P} < 1$. Meanwhile, the probability that *Algorithm* 1 can get a solution whose cost is less than $\varepsilon \cdot \mathcal{C}_{\text{s-MILP}}$ within $M$ iterations is $1 - \mathbf{P}^M$. Therefore, we have $\lim_{M \to +\infty} \left(1 - \mathbf{P}^M\right) = 1$, and have proven that *Algorithm* 1 can converge to ensure a bounded approximation ratio (*i.e.*, $\varepsilon$). ■

*1)* ***Probabilistic Approximation of Algorithms****:* In *Algorithms* 1 and 2, we get a feasible integer solution from the real solution of LP with randomized rounding. To avoid generating a large number of infeasible solution in the process, we do not round $\{C_{m,v}^{\text{LC}}, C_{n,v}^{\text{EC}}, C_{k,v}^{\text{L-EC}}\}$ directly, but compute their values by rounding $\{y_{m,v}^i, x_{n,v}^i\}$, *i.e.*, *Lines* 2-4 in *Algorithm* 1 ensure that feasible $\{C_{m,v}^{\text{LC}}, C_{n,v}^{\text{EC}}, C_{k,v}^{\text{L-EC}}\}$ can be calculated.

We denote the total cost and cost of allocated LCs/ECs/L-ECs obtained in each iteration of *Algorithm* 1 or 2 as $\hat{\mathcal{C}}$, $\mathcal{C}_{\text{LC}}$, $\mathcal{C}_{\text{EC}}$ and $\mathcal{C}_{\text{L-EC}}$, respectively. Then, the expectation of the total cost can be calculated as follows, where $\{\bullet^*\}$ refer to the real value obtained by solving the LP in *Line* 4 of *Algorithm* 1.

$$\begin{aligned}\mathbb{E}(\hat{\mathcal{C}}) &= \mathbb{E}(\mathcal{C}_{\text{LC}}) + \mathbb{E}(\mathcal{C}_{\text{EC}}) + \mathbb{E}(\mathcal{C}_{\text{L-EC}}) \\ &\leq \sum_{m,v} [\mathbb{P}(C_{m,v}^{\text{LC}} = 1) \cdot \alpha_m] + \sum_{n,v} \mathbb{P}[(C_{n,v}^{\text{EC}} = 1) \cdot \beta_n].\end{aligned} \tag{55}$$

where $\{C^{\text{LC}}_{m,v}, C^{\text{EC}}_{n,v}\}$ refers to the allocation of LCs/ECs before we replace bundles of LCs/ECs with L-ECs. Then, we have

$$\begin{aligned}&\sum_{v}\mathbb{P}(C^{\text{LC}}_{m,v}=1)\le\sum_{v}\mathbb{P}\left[1-\prod_{r_i}(1-y^i_{m,v})=1\right]\\&=\sum_{v}\mathbb{P}\left[\prod_{r_i}(1-y^i_{m,v})=0\right]\le\sum_{v,r_i}\mathbb{P}(y^i_{m,v}=1)\\&\le\sum_{v,r_i}y^{i*}_{m,v}+\sum_{v',r_i}\mathbb{P}(y^i_{m,v'}=1)\cdot y^{i\circ}_{m,v'},\end{aligned}\tag{56}$$

where $v'$ denotes a node on which flow $r_i$ might need to go across fiber trees, and $y^{i\circ}_{m,v'}$ is defined as

$$y^{i\circ}_{m,v'}=\frac{1-\sum\limits_{m}y^{i*}_{m,v'}}{\sum\limits_{m}\tilde{y}^i_{m,v'}},$$

where $\tilde{y}^i_{m,v'}$ is defined as

$$\tilde{y}^i_{m,v'}=\begin{cases}1, & y^{i*}_{m,v'}>0,\\0, & \text{otherwise},\end{cases}\quad\forall r_i,\ v',\ m\in[1,N].$$

Therefore, Eq. (56) can be derived with

$$\begin{aligned}&\sum_{v',r_i}\mathbb{P}(y^i_{m,v'}=1)\cdot y^{i\circ}_{m,v'}\le\\&\sum_{r_i,v,k}\mathbb{P}\left[\sum_{(u,v)}Z^i_{(u,v)}\cdot P_{(u,v),k}=1,\sum_{(v,p)}Z^i_{(v,p)}\cdot(1-P_{(v,p),k})=1\right]\\&\cdot y^{i\circ}_{m,v}\le\\&\sum_{r_i,v,k}\left[\sum_{(u,v)}Z^{i\circ}_{(u,v)}\cdot P_{(u,v),k}\right]\left[\sum_{(v,p)}Z^{i\circ}_{(v,p)}\cdot(1-P_{(v,p),k})\right]\cdot y^{i\circ}_{m,v},\end{aligned}$$

where $Z^{i\circ}_{(u,v)}$ is defined as

$$Z^{i\circ}_{(u,v)}=\frac{1-\sum\limits_{(u,p)}Z^{i*}_{(u,p)}}{\sum\limits_{(u,p)}\tilde{Z}^i_{(u,p)}}+Z^{i*}_{(u,v)},$$

where $\tilde{Z}^i_{(u,p)}$ is defined as

$$\tilde{Z}^i_{(u,p)}=\begin{cases}1, & Z^{i*}_{(u,p)}>0,\\0, & \text{otherwise},\end{cases}\quad\forall r_i\in\mathcal{R},\ (u,p)\in E.$$

Similarly, we have

$$\begin{aligned}&\sum_{v}\mathbb{P}(C^{\text{EC}}_{n,v}=1)\le\sum_{r_i,v}x^{i*}_{n,v}+\\&\sum_{r_i,k}\left\{\sum_{(u,v)}Z^{i^\circ}_{(u,v)}P_{(u,v),k}\left\{1-\prod_{p\in V}\left[1-T_{p,k}(1-t_{s,p})\right]\right\}\right\}x^{i\circ}_{n,s_i},\end{aligned}\tag{57}$$

where we define $x^{i\circ}_{n,s_i}$ as

$$x^{i\circ}_{n,s_i}=\frac{1-\sum\limits_{n}x^{i*}_{n,s_i}}{\sum\limits_{n}\tilde{x}^i_{n,s_i}},$$

where $\tilde{x}^i_{n,s_i}$ is defined as

$$\tilde{x}^i_{n,s_i}=\begin{cases}1, & x^{i*}_{n,s_i}>0,\\0, & \text{otherwise},\end{cases}\quad\forall r_i\in\mathcal{R},\ n\in[1,N].$$

With the aforementioned derivation (especially Eqs. (56) and (57)), we can obtain the upper-bound of the expectation of the total cost $\mathbb{E}(\hat{\mathcal{C}})$ in each iteration of *Algorithm* 1 or 2 and the upper-bound of the value of $\sum_{m,v}[\mathbb{P}(C^{\text{LC}}_{m,v}=1)\cdot\alpha^2_m]+\sum_{n,v}\mathbb{P}[(C^{\text{EC}}_{n,v}=1)\cdot\beta^2_n]$ which is used follows. Then, we can apply **Theorem** 3 below to estimate the upper-bound of the probability that *Algorithm* 1 cannot find a feasible solution, which satisfies a preset approximation ratio $\varepsilon\ge1$.

**Theorem 3.** *Let $S=\sum\limits_{i}a_i\cdot X_i$, where $\{X_i\}$ are possibly-dependent random binary variables and each $a_i\in\mathbb{R}$. If we define $x_i=\mathbb{E}[X_i]$, the randomized rounding algorithm, which gets $X_i\in\{0,1\}$ based on a given set of $\{x_i\}$, satisfies [51]:*

$$\mathbb{P}(S-\mathbb{E}(S)\ge t)\le\exp\left\{-\frac{t^2}{2\varphi\left[\sum\limits_{i}a^2_i(x_i-x^2_i)+\frac{Mt}{3}\right]}\right\},\tag{58}$$

*where $M=\max\limits_{i}(|a_i|)$, $t\ge0$, and $\varphi\ge1$.*

According to Eq. (55), we have

$$\mathbb{E}(\hat{\mathcal{C}})\le\sum_{m,v}[\mathbb{P}(C^{\text{LC}}_{m,v}=1)\cdot\alpha_m]+\sum_{n,v}[\mathbb{P}(C^{\text{EC}}_{n,v}=1)\cdot\beta_n].$$

Then, we set $\{a_i\}=\{\overbrace{\alpha_m,\cdots,\alpha_m}^{|V||N|},\overbrace{\beta_n,\cdots,\beta_n}^{|V||N|}\}$, $\{x_i\}=\{\{\mathbb{P}(C^{\text{LC}}_{m,v}=1),\forall v\in V,m\in[1,N]\},\{\mathbb{P}(C^{\text{EC}}_{n,v}=1),\forall v\in V,n\in[1,N]\}\}$, $\varphi=1$, and $t=\varepsilon\cdot\mathcal{C}_{\text{LP}}$, where $\mathcal{C}_{\text{LP}}$ is the solution of the LP (*i.e.*, a lower-bound of s-MILP). Hence, by putting these into Eq. (58) in *Theorem* 3, we have

$$\mathbb{P}\left(\hat{\mathcal{C}}-\mathbb{E}(\hat{\mathcal{C}})\ge\varepsilon\cdot\mathcal{C}_{\text{LP}}\right)\le\exp\left(-\frac{(\varepsilon\cdot\mathcal{C}_{\text{LP}})^2}{2\left[\sum\limits_{i}a^2_ix_i+\frac{M\mathcal{C}_{\text{LP}}}{3}\right]}\right).$$

As we always have $\mathcal{C}_{\text{s-MILP}}\ge\mathcal{C}_{\text{LP}}$, we can further get

$$\mathbb{P}\left(\hat{\mathcal{C}}-\mathbb{E}(\hat{\mathcal{C}})\ge\varepsilon\cdot\mathcal{C}_{\text{s-MILP}}\right)\le\exp\left(-\frac{(\varepsilon\cdot\mathcal{C}_{\text{LP}})^2}{2\left[\sum\limits_{i}a^2_ix_i+\frac{M\mathcal{C}_{\text{LP}}}{3}\right]}\right)=\mathbf{P},$$

where $\mathcal{C}_{\text{LP}}$, $\mathbb{E}(\hat{\mathcal{C}})$, $\sum\limits_{i}a^2_ix_i=\sum_{m,v}[\mathbb{P}(C^{\text{LC}}_{m,v}=1)\cdot\alpha^2_m]+\sum_{n,v}\mathbb{P}[(C^{\text{EC}}_{n,v}=1)\cdot\beta^2_n]$ can be obtained by solving the LP, $M=\max\left(\max\limits_{m}(\alpha_m),\max\limits_{n}(\beta_n)\right)$. Therefore, the probability that *Algorithm* 1 can solve s-MILP to satisfy a preset approximation ratio $\varepsilon$ is at least $1-\mathbf{P}^{Q_1\cdot Q_2}$.

*2) **Complexity Analysis of Algorithms**:* The iterations in *Algorithm* 1 or 2 will stop when $Q_1$ or $Q_2$ is reached. In *Algorithm* 1, the LP solving in *Lines* 1-4 can be accomplished in polynomial-time [52], and the time complexity of *Lines* 5-23 is $O(Q_1\cdot(|V|\cdot|\mathcal{R}|\cdot N+Q_2\cdot(|\mathcal{R}|\cdot|V|^2+|\mathcal{R}|\cdot|V|\cdot N^2)))$. Hence, *Algorithm* 1 is a polynomial-time approximation algorithm.

## V. Performance Evaluation

In this section, we present numerical simulation results to demonstrate the effectiveness of our proposals.

### A. Simulation Setup

The simulations consider three real-world physical topologies as shown in Fig. 4, which are the Italian Network, Netrail, and NSFNET. As FONs are usually used for metro-aggregation networks, the topologies are modified from their

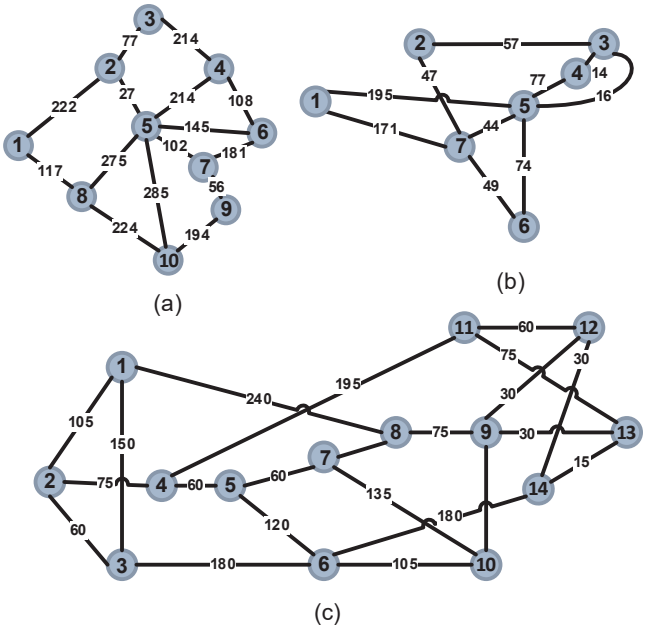


Fig. 4. Physical topologies considered in simulations: (a) Italian Network, (b) Netrail, and (c) NSFNET (fiber link lengths are marked in kilometers).

**Algorithm 3:** Heuristic (adapted from [16])

**Input**: Parameters of w-MILP.
**Output**: Establishment of fiber trees $T$, allocation of LCs/ECs/L-ECs, total cost $\mathcal{C}$.

1 generate initial fiber trees $T$ based on physical topology of FON and flows in $\mathcal{R}$;
2 provision flows in $\mathcal{R}$ based on $T$, allocate LCs/ECs and calculate the total cost $\mathcal{C}$ accordingly;
3 initialize $E' = E$, and remove links in $T$ from $E'$;
4 **for** *each link in* $E'$ **do**
5 insert the link in a proper fiber tree or mark it as a new fiber tree based on $T$ to obtain a new set $T'$;
6 repeat *Line* 2 to provision flows in $\mathcal{R}$ based on $T'$;
7 **if** *the total cost* $\mathcal{C}$ *is reduced* **then**
8 set $T = T'$, and update the allocated LCs/ECs and the total cost $\mathcal{C}$ accordingly;
9 **end**
10 **end**
11 replace each bundle of LC and EC with an L-EC, and update the planned FON and total cost $\mathcal{C}$;

original versions to scale down the link lengths if necessary. We assume that the bandwidth demand of each flow $r_i \in \mathcal{R}$ is randomly distributed within $[25, 200]$ Gbps. According to the values reported in the literature [11, 13–15], we assume that the set of feasible capacities of LCs/ECs/L-ECs is $B^c = \{40, 100, 400\}$ Gbps. Meanwhile, the unit costs of the LCs, ECs and L-ECs with a capacity of $\{40, 100, 400\}$ Gbps are set as $\{1, 2, 4\}$, $\{2, 4, 6\}$ and $\{2.5, 5, 8\}$, respectively [11, 12, 16]. The maximum number of LCs/ECs/L-ECs that can be deployed on each node (*i.e.*, $N$) and the capacity of each feasible LC/EC/L-EC (*i.e.*, $\{b_n^c,\ \forall n \in [1, N]\}$ are set according to the actual traffic condition in each simulation.

We evaluate four algorithms, which are 1) the one that directly solves w-MILP in Section III-B (w-MILP), 2) the one that solves the optimization in Section IV-A for fiber tree establishment and directly solves s-MILP in Section IV-B for allocation of LCs/ECs/L-ECs (FT/s-MILP), 3) the one that solves the optimization in Section IV-A for fiber tree establishment and solves s-MILP with *Algorithm* 1 for allocation of LCs/ECs/L-ECs (FT/Approx), and 4) a heuristic by modifying the one designed in [16] (Heuristic). The procedure of Heuristic is shown in *Algorithm* 3. Specifically, we first generate a few initial fiber trees (*Line* 1), then provision flows based on the initial fiber trees (*Line* 2), and next update the fiber trees and flow provision schemes iteratively to reduce the total cost of deployed LCs/ECs (*Lines* 3-10), and finally, in *Line* 11, we replace each bundle of LC and EC with an L-EC and update the planned FON and its total cost.

The simulations of w-MILP, FT/s-MILP and FT/Approx are conducted on a computer with 2.2 GHz Intel Xeon Silver 4210 CPU and 128 GB memory, and the environment is Clion 3.19 with Gurobi 9.1.1 [53]. The simulations of Heuristic run on a computer with 2.1 GHz Intel Xeon Silver 4110 CPU and 32 GB memory, and the environment is MATLAB 2019a. To ensure sufficient statistical accuracy, we average the results from 5 independent runs to get each data point in the simulations. Note that, as the fiber tree establishment is based on the weight defined in Eq. (49), which depends on the flows in $\mathcal{R}$, each run can build the FON with different fiber trees.

### B. Small-Scale Simulations

The small-scale simulations use the 7-node Netrail topology to compare the performance of all the four algorithms. In this scenario, we first set the maximum number of LCs/ECs/L-ECs that can be allocated on a node (*i.e.*, $N$) to be big enough, assume the maximum hop that a lightpath can be transmitted within a fiber tree before being received as $h_{\max} = 10$, and then change the values of $N$ and $h_{\max}$ respectively to evaluate their impacts. We set the longest running time of each algorithm to be 2 hours, and then w-MILP and FT/s-MILP can be solved when the problem scales are $|\mathcal{R}| \leq 14$ and $|\mathcal{R}| \leq 22$, respectively. As for FT/Approx, we verify with simulations that it can obtain a near-optimal solution of s-MILP easily. For example, if we set $\varepsilon = 1$, the results show that the probability, with which *Algorithm* 1 gets a solution whose cost is greater than $\mathcal{C}_{\text{s-MILP}}$ in each iteration, is $\mathbf{P} \leq 0.17$.

Fig. 5 compares the total costs from all the algorithms when we have $|\mathcal{R}| \leq 14$, where for each number of flows, we plot four bars to denote the total costs from w-MILP, FT/s-MILP, FT/Approx and Heuristic, respectively, and in each bar, we mark the costs from LCs, ECs and L-ECs in different colors. FT/s-MILP can always provide the same solutions as the exact ones from w-MILP. The total costs from FT/Approx are always close to the optimal ones from w-MILP and FT/s-MILP, and they are much smaller than those from Heuristic when we have $|\mathcal{R}| \geq 10$. Meanwhile, we can see that the distributions of used LCs/ECs/L-ECs provided by w-MILP and FT/s-MILP are always the same, those from FT/Approx are similar to them, but those from Heuristic are significantly different. Therefore,

TABLE I
PERFORMANCE OF FOUR ALGORITHMS: W-MILP, FT/S-MLIP, FT/APPROX AND HEURISTIC IN NETRAIL

| | Running Time per Flow (seconds) | | | | Average Path Length (km) | | | | Max Hops in a Fiber Tree | | | | Used Fiber Trees per Flow | | | |
|---|---|---|---|---|---|---|---|---|---|---|---|---|---|---|---|---|
| Number of Flows | 8 | 10 | 12 | 14 | 8 | 10 | 12 | 14 | 8 | 10 | 12 | 14 | 8 | 10 | 12 | 14 |
| w-MILP | 27.52 | 58.89 | 73.32 | 238.49 | 147 | 158.30 | 104.58 | 132.29 | 3 | 3 | 2 | 2 | 1.90 | 1.90 | 1.50 | 1.43 |
| FT/s-MILP | 2.27 | 3.38 | 3.91 | 4.95 | 147 | 158.30 | 104.58 | 132.29 | 3 | 3 | 2 | 2 | 1.90 | 1.90 | 1.50 | 1.43 |
| FT/Approx | 0.51 | 0.64 | 0.82 | 0.99 | 147 | 158.30 | 104.58 | 125.93 | 3 | 3 | 2 | 2 | 1.90 | 1.90 | 1.50 | 1.50 |
| Heuristic | 0.03 | 0.04 | 0.04 | 0.04 | 111.5 | 123.50 | 115.67 | 127.93 | 3 | 1 | 1 | 3 | 1.38 | 1.50 | 1.83 | 1.93 |

TABLE II
DEPLOYED OTN ENCRYPTION ARCHITECTURES IN NETRAIL

| Number of Flows | Deployed OTN Encryption Architectures | | | |
|---|---|---|---|---|
| | w-MILP | FT/s-MILP | FT/Approx | Heuristic |
| 8 | *Flow* 2 *Architecture* IV<br>Others: No Encryption | *Flow* 2: *Architecture* IV<br>Others: No Encryption | *Flow* 2: *Architecture* IV<br>Others: No Encryption | *Flow* 5: *Architecture* III<br>Others: No Encryption |
| 10 | *Flow* 2: *Architecture* IV<br>*Flow* 6: *Architecture* III<br>Others: No Encryption | *Flow* 2: *Architecture* IV<br>*Flow* 6: *Architecture* III<br>Others: No Encryption | *Flow* 2: *Architecture* IV<br>*Flow* 6: *Architecture* III<br>Others: No Encryption | *Flow* 3: *Architecture* I<br>*Flow* 6: *Architecture* I<br>Others: No Encryption |
| 12 | *Flow* 10: *Architecture* IV<br>Others: No Encryption | *Flow* 10: *Architecture* IV<br>Others: No Encryption | *Flow* 10: *Architecture* IV<br>Others: No Encryption | *Flow* 4: *Architecture* I<br>*Flow* 6: *Architecture* III<br>*Flow* 9: *Architecture* III<br>*Flow* 10: *Architecture* I<br>Others: No Encryption |
| 14 | *Flow* 4: *Architecture* I<br>*Flow* 6: *Architecture* III<br>Others: No Encryption | *Flow* 4: *Architecture* I<br>*Flow* 6: *Architecture* III<br>Others: No Encryption | *Flow* 4: *Architecture* IV<br>*Flow* 6: *Architecture* III<br>Others: No Encryption | *Flow* 6: *Architecture* III<br>*Flow* 10: *Architecture* I<br>*Flow* 12: *Architecture* III<br>*Flow* 13: *Architecture* III<br>Others: No Encryption |

TABLE III
PERFORMANCE OF THREE ALGORITHMS: FT/S-MLIP, FT/APPROX AND HEURISTIC IN NETRAIL

| | Running Time per Flow (seconds) | | | | Average Path Length (km) | | | | Max Hops in a Fiber Tree | | | |
|---|---|---|---|---|---|---|---|---|---|---|---|---|
| Number of Flows | 16 | 18 | 20 | 22 | 16 | 18 | 20 | 22 | 16 | 18 | 20 | 22 |
| FT/s-MILP | 9.19 | 14.04 | 31.73 | 215.35 | 123.15 | 134.28 | 122.35 | 139.18 | 2 | 2 | 2 | 2 |
| FT/Approx | 7.18 | 8.79 | 21.08 | 32.72 | 117.56 | 128.78 | 121.35 | 120.78 | 2 | 2 | 2 | 2 |
| Heuristic | 0.04 | 0.05 | 0.05 | 0.05 | 121.33 | 117.00 | 123.15 | 154.68 | 1 | 1 | 2 | 2 |

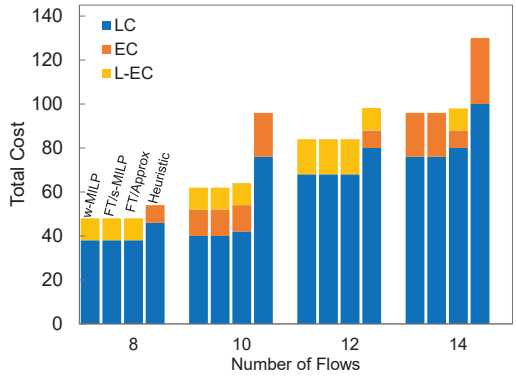


Fig. 5. Total costs from all the algorithms in Netrail.

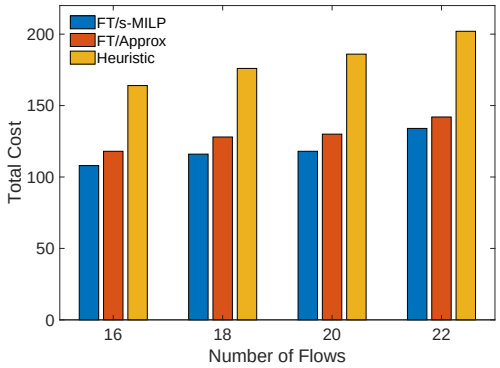


Fig. 6. Total costs from FT/s-MLIP, FT/Approx and Heuristic in Netrail.

the results in Fig. 5 suggest that for such small-scale multilayer planning for FON with OTN encryption, the arrangement of FT/s-MILP does not bring in any performance loss related to solving w-MILP directly, and FT/Approx can approximate the optimal solutions well. Table I shows the results on running time per flow, average path length of flows, maximum hops that each flow goes across in a fiber tree, and average fiber trees used by each flow, which further verifies the effectiveness

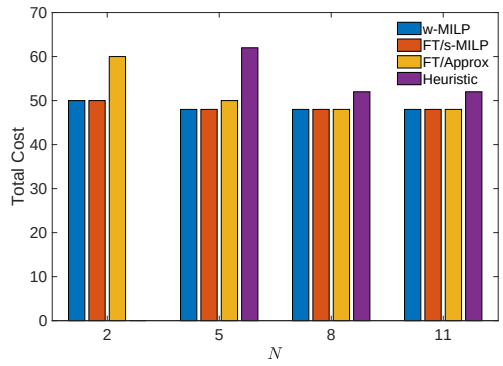


Fig. 7. Total costs with different values of $N$ (in Netrail and $|\mathcal{R}| = 8$).

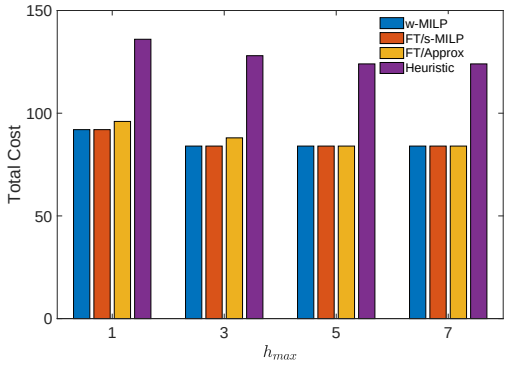


Fig. 8. Total costs with different values of $h_{\max}$ (in Netrail and $|\mathcal{R}| = 8$).

of FT/s-MILP and FT/Approx. As expected, Heuristic runs the fastest and FT/Approx is the second most time-efficient one.

Table II lists the OTN encryption architectures selected by the algorithms for flows in Netrail, which are obtained by analyzing each planned FON manually. To save space, we, for each $|\mathcal{R}|$, only show the results of one set of flows, but have confirmed that those of other sets follow similar trends. Note that, the security-aware multilayer planning does not need to encrypt a flow if it is provisioned in the way that its lightpath will not be received by any node (except for its own destination) that does not have mutual trustiness with its source. The results in Table II suggest that FT/s-MILP and FT/Approx always select similar architectures as w-MILP while Heuristic performs significantly different from them. This further verifies the superiority of our proposals.

If we increase the problem scale beyond $|\mathcal{R}| = 14$, w-MILP becomes intractable. Hence, Fig. 6 shows the total costs from FT/s-MILP, FT/Approx, and Heuristic, when we have $|\mathcal{R}| \in [16, 22]$, and Table III still lists the running time per flow, average path length of flows, and maximum hops that each flow goes across in a fiber tree of the three algorithms. Similar trends as those in Fig. 5 and Table I can still be observed.

Next, we investigate the impacts of $N$ and $h_{\max}$ by fixing the problem scale as $|\mathcal{R}| = 8$. Fig. 7 shows the algorithms' performance under different $N$. Note that, Heuristic cannot deliver a feasible solution with $N = 2$ because the greedy idea behind it leads to more LCs/ECs/L-ECs usages, which is the reason why we only show the results from the other three algorithms for this case in Fig. 7. We observe that changing the value of $N$ does not affect the fact that FT/s-MILP does not bring in any performance loss related to solving w-MILP directly, and the performance of FT/Approx and Heuristic first gets improved and then stays unchanged when $N$ increases. This is because when there are only very few feasible LCs/ECs/L-ECs on each node, FT/Approx and Heuristic may serve each flow with more lightpaths for making detours. When $N$ increases (*i.e.*, more LCs/ECs/L-ECs can be allocated on each node), FT/Approx and Heuristic can make less detours to find feasible LCs/ECs/L-ECs for flows. However, as the number of flows in $\mathcal{R}$ are fixed for all the simulation scenarios considered in Fig. 7, FT/Approx and Heuristic cannot further reduce the total cost after $N$ reaches 8. Meanwhile, because Heuristic cannot optimize the security-aware multilayer planning as good as our proposed algorithms, there does not exist a value of $N$, for which it can deliver the same total cost as those from our proposed algorithms.

TABLE IV
RUNNING TIME PER FLOW (IN NETRAIL AND $|\mathcal{R}| = 8$)

| Number of Feasible LCs/ECs/L-ECs on each Node ($N$) | Running Time per Flow (seconds) | | | |
|---|---|---|---|---|
| | w-MILP | FT/s-MILP | FT/Approx | Heuristic |
| 2 | 19.57 | 0.32 | 0.03 | – |
| 5 | 24.01 | 0.77 | 0.14 | 0.03 |
| 8 | 26.34 | 2.02 | 0.49 | 0.03 |
| 11 | 28.67 | 2.59 | 0.53 | 0.04 |

Table IV shows the running time of the algorithms. We can see that a smaller $N$ leads to shorter running time for w-MILP, FT/s-MILP and FT/Approx, which is because a smaller $N$ corresponds to a small solution space to search. Fig. 8 illustrates the impact of $h_{\max}$. We can see that the performance of FT/Approx and Heuristic first improves with the increase of $h_{\max}$. This is because a larger $h_{\max}$ allows more routing options for each flow, *i.e.*, the optimization space for each algorithm is larger. However, the performance of FT/Approx and Heuristic cannot be further improved when $h_{\max}$ reaches 5, because longer lightpaths might not be used for flows anyway. To further analyze the impacts of $N$ and $h_{\max}$, we increase the problem scale to $|\mathcal{R}| = 12$ and redo the simulations. Figs. 9 and 10 show the algorithms' performance under different values of $N$ and $h_{\max}$, respectively, and similar trends can be observed as those in Figs. 7 and 8.

### C. Large-Scale Simulations

The large-scale simulations consider the physical topologies of Italian Network and NSFNET, and due to the time complexity of w-MILP and FT/s-MILP, we only simulate FT/Approx and Heuristic. The total costs with Italian Network are shown in Fig. 11, which indicates that FT/Approx can still achieve more cost-effective multilayer planning for FONs with OTN encryption than Heuristic, realizing a cost saving within $[21\%, 48\%]$. The algorithms' running time is listed in Table

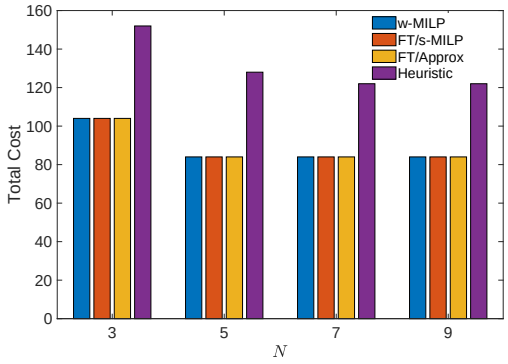


Fig. 9. Total costs with different values of $N$ (in Netrail and $|\mathcal{R}| = 12$).

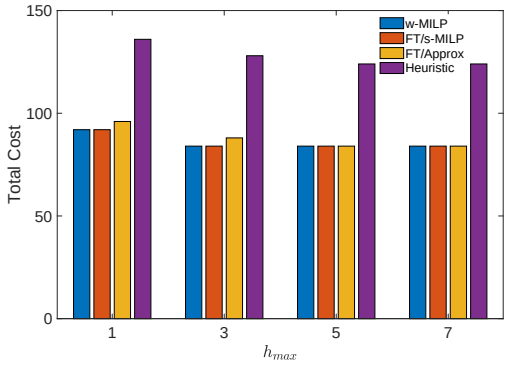


Fig. 10. Total costs with different values of $h_{\max}$ (in Netrail and $|\mathcal{R}| = 12$).

V. We can see that FT/Approx does take more time to run, but the majority of its running time gets spent on solving the two LPs in *Algorithm* 1 (*Lines* 1-4), which means that the iterations for randomized rounding run very time-efficiently.

This analysis can be further verified with the convergence performance of FT/Approx in Fig. 12, where the red line shows the expected total cost with $\varepsilon = 2$ for terminating the iterations (*i.e.*, $\hat{\mathcal{C}} \leq 2 \cdot \mathcal{C}_{\text{LP}} + \mathbb{E}(\hat{\mathcal{C}})$). FT/Approx runs for $\sim$4200 iterations to make the total cost go below the expected one. After reaching the expected total cost for terminating the iterations, FT/Approx continues to optimize the objective, further verifying its effectiveness. Fig. 13 and Table VI show the simulation results with NSFNET, and similar trends can be observed as those in Fig. 11 and Table V, respectively. Specifically, in Fig. 13, the cost saving achieved by FT/Approx over Heuristic is within $[16\%, 68\%]$.

TABLE V
RUNNING TIME PER FLOW IN ITALIAN NETWORK

| Number of Flows | Running Time per Flow (seconds) | | |
|---|---|---|---|
| | FT/Approx | | Heuristic |
| | Total | Solving LPs | |
| 20 | 8.26 | 2.15 | 0.08 |
| 40 | 10.30 | 5.49 | 0.17 |
| 60 | 10.95 | 9.29 | 0.23 |
| 80 | 16.24 | 15.10 | 0.24 |

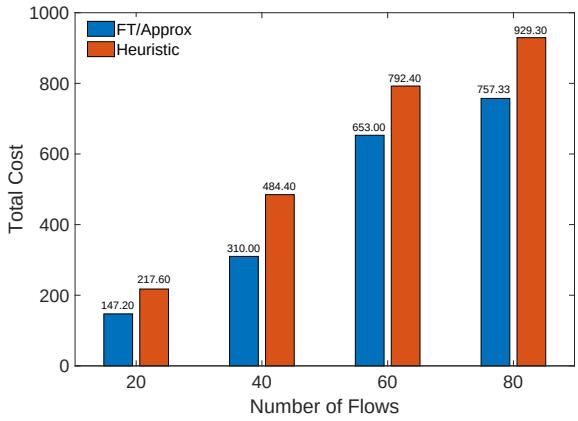


Fig. 11. Total cost in Italian Network.

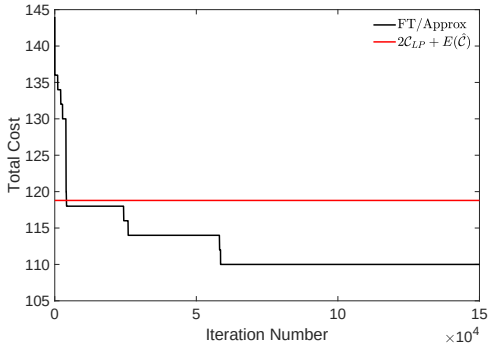


Fig. 12. Convergence of FT/Approx for $|\mathcal{R}| = 20$ in Italian Network.

## VI. CONCLUSION

In this paper, we proposed to leverage OTN encryption to enhance the security in FONs. In order to tackle the resulting security-aware multilayer planning, we first formulated an MILP model (namely, w-MILP) to solve the problem exactly. Then, to reduce the time complexity of problem-solving, we transformed w-MILP into two correlated MILP models for establishing fiber trees for an FON (t-MILP) and provisioning flows in the fiber trees (s-MILP), respectively.

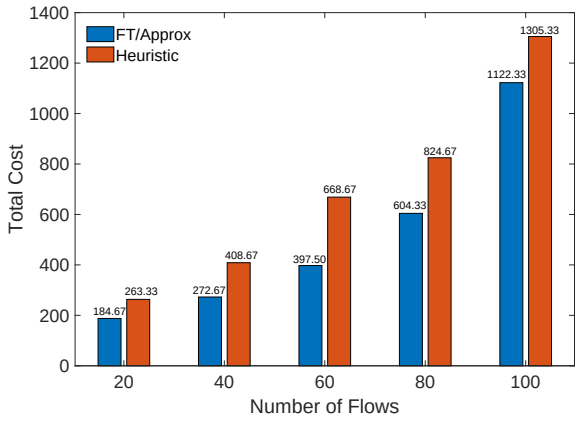


Fig. 13. Total cost in NSFNET.

TABLE VI
RUNNING TIME PER FLOW IN NSFNET

| Number of Flows | Running Time per Flow (seconds) | | |
|---|---|---|---|
| | FT/Approx | | Heuristic |
| | Total | Solving LPs | |
| 20 | 2.08 | 1.01 | 0.20 |
| 40 | 2.64 | 2.03 | 0.20 |
| 60 | 11.97 | 4.79 | 0.33 |
| 80 | 20.99 | 19.46 | 0.39 |
| 100 | 23.44 | 22.37 | 0.48 |

The optimization in t-MILP was modeled as a weighted set partitioning problem and solved time-efficiently. As for s-MILP, we proposed a polynomial-time approximation algorithm to solve it based on LP relaxation and randomized rounding. Extensive simulations confirmed that our proposals can take security requirements into consideration to plan FONs with OTN encryption cost-effectively.

## ACKNOWLEDGMENTS

This work was supported by NSFC project 61871357 and Fundamental Fund for Central Universities (WK3500000006).

## REFERENCES

[1] "Cisco Annual Internet Report (2018-2023)," *Online White Report*. [Online]. Available: https://www.cisco.com/c/en/us/solutions/collateral/executive-perspectives/annual-internet-report/white-paper-c11-741490.html.

[2] P. Lu, L. Zhang, and X. Liu, "Highly-efficient data migration and backup for big data applications in elastic optical inter-data-center networks," *IEEE Netw.*, vol. 29, pp. 36–42, Sept./Oct. 2015.

[3] M. Filer *et al.*, "Low-margin optical networking at cloud scale," *J. Opt. Commun. Netw.*, vol. 11, pp. C94–C108, Oct. 2019.

[4] Z. Zhu, W. Lu, L. Zhang, and N. Ansari, "Dynamic service provisioning in elastic optical networks with hybrid single-/multi-path routing," *J. Lightw. Technol.*, vol. 31, pp. 15–22, Jan. 2013.

[5] L. Gong *et al.*, "Efficient resource allocation for all-optical multicasting over spectrum-sliced elastic optical networks," *J. Opt. Commun. Netw.*, vol. 5, pp. 836–847, Aug. 2013.

[6] L. Gong and Z. Zhu, "Virtual optical network embedding (VONE) over elastic optical networks," *J. Lightw. Technol.*, vol. 32, pp. 450–460, Feb. 2014.

[7] J. Liu *et al.*, "On dynamic service function chain deployment and readjustment," *IEEE Trans. Netw. Serv. Manag.*, vol. 14, no. 3, pp. 543–553, Sept. 2017.

[8] L. Gong, Y. Wen, Z. Zhu, and T. Lee, "Toward profit-seeking virtual network embedding algorithm via global resource capacity," in *Proc. of INFOCOM 2014*, pp. 1–9, Apr. 2014.

[9] V. Dukic *et al.*, "Beyond the mega-data center: networking multi-data center regions," in *Proc. of ACM SIGCOMM 2020*, pp. 765–781, Aug. 2020.

[10] C. Tremblay *et al.*, "Filterless optical networks: a unique and novel passive WAN network solution," in *Proc. of OECC/IOOC 2007*, pp. 466–467, Jul. 2007.

[11] J. Ceballos, R. DiPasquale, and R. Feldman, "Business continuity and security in datacenter interconnection," *Bell Labs Tech. J.*, vol. 17, pp. 147–155, Jul. 2012.

[12] F. Chen, M. Song, F. Zhou, and Z. Zhu, "Security-aware planning of packet-over-optical networks in consideration of OTN encryption," *IEEE Trans. Netw. Serv. Manag.*, vol. 18, pp. 3209–3220, Sept. 2021.

[13] K. Guan, J. Kakande, and J. Cho, "On deploying encryption solutions to provide secure transport-as-a-service (TaaS) in core and metro networks," in *Proc. of ECOC 2016*, pp. 1–3, Sept. 2016.

[14] "High-capacity wire-speed encryption modules for the 6500 packet-optical platform," *Technical Report*. [Online]. Available: https://www.ciena.com/products/high-capacity-wire-speed-encryption-modules/.

[15] "mTera ODU payload encryption: Wire-speed encryption with the flexibility of universal switching," *Online Technical Report*. [Online]. Available: https://www.infinera.com/wp-content/uploads/mTera-ODU-Payload-Encryption-0008-AN-RevA-0419.pdf.

[16] Q. Lv and Z. Zhu, "Planning security-aware filterless optical networks," in *Proc. of ACP 2021*, pp. 1–3, Oct. 2021.

[17] F. Abtahi *et al.*, "Optimal design of cost-and energy-efficient scalable passive optical backbone networks," in *Proc. of ACP 2012*, pp. 1–3, Nov. 2012.

[18] O. Ayoub *et al.*, "Tutorial on filterless optical networks," *J. Opt. Commun. Netw.*, vol. 14, pp. 1–15, Mar. 2022.

[19] M. Ruiz, O. Pedrola, L. Velasco, and D. Careglio, "Survivable IP/MPLS-over-WSON multilayer network optimization," *J. Opt. Commun. Netw.*, vol. 3, pp. 1629–640, Aug. 2011.

[20] W. Shi, Z. Zhu, M. Zhang, and N. Ansari, "On the effect of bandwidth fragmentation on blocking probability in elastic optical networks," *IEEE Trans. Commun.*, vol. 61, pp. 2970–2978, Jul. 2013.

[21] V. Gkamas, K. Christodoulopoulos, and E. Varvarigos, "A joint multilayer planning algorithm for IP over flexible optical networks," *J. Lightw. Technol.*, vol. 33, pp. 2965–2977, Jul. 2015.

[22] W. Lu, X. Yin, X. Cheng, and Z. Zhu, "On cost-efficient integrated multilayer protection planning in IP-over-EONs," *J. Lightw. Technol.*, vol. 35, pp. 5335–5346, Dec. 2017.

[23] X. Chen *et al.*, "Deep-RMSA: A deep-reinforcement-learning routing, modulation and spectrum assignment agent for elastic optical networks," in *Proc. of OFC 2018*, pp. 1–3, Mar. 2018.

[24] S. Liu, W. Lu, and Z. Zhu, "On the cross-layer orchestration to address IP router outages with cost-efficient multilayer restoration in IP-over-EONs," *J. Lightw. Technol.*, vol. 10, pp. A122–A132, Jan. 2018.

[25] P. Pavon-Marino *et al.*, "On the benefits of point-to-multipoint coherent optics for multilayer capacity planning in ring networks with varying traffic profiles," *J. Opt. Commun. Netw.*, vol. 14, pp. B30–B44, May 2022.

[26] M. Hosseini *et al.*, "Optimization of survivable filterless optical networks exploiting digital subcarrier multiplexing," *J. Opt. Commun. Netw.*, vol. 14, pp. 586–594, Jul. 2022.

[27] M. Fok, Z. Wang, Y. Deng, and P. Prucnal, "Optical layer security in fiberoptic network," *IEEE Trans. Inf. Forensics Secur.*, vol. 6, pp. 725–736, Sept. 2011.

[28] M. Furdek, N. Skorin-Kapov, and M. Grbac, "Attack-aware wavelength assignment for localization of in-band crosstalk attack propagation," *J. Opt. Commun. Netw.*, vol. 2, pp. 1000–1009, Nov. 2010.

[29] J. Zhu, B. Zhao, and Z. Zhu, "Attack-aware service provisioning to enhance physical-layer security in multi-domain EONs," *J. Opt. Commun. Netw.*, vol. 34, pp. 2645–2655, Jun. 2016.

[30] Q. Lv, F. Zhou, and Z. Zhu, "On the bilevel optimization to design control plane for SDONs in consideration of planned physical-layer attacks," *IEEE Trans. Netw. Serv. Manag.*, vol. 18, pp. 3221–3230, Sept. 2021.

[31] X. Jin, W. Lu, S. Liu, and Z. Zhu, "On multi-layer restoration in optical networks with encryption solution deployment," in *Proc. of OFC 2018*, pp. 1–3, Mar. 2018.

[32] P. Pavon-Marino *et al.*, "Techno-economic impact of filterless a plane and agile control plane in the 5G optical metro," *J. Lightw. Technol.*, vol. 38, pp. 3801–3814, Aug. 2020.

[33] O. Karandin, O. Ayoub, F. Musumeci, and M. Tornatore, "A techno-economic comparison of filterless and wavelength-switched optical metro networks," in *Proc. of ICTON 2020*, pp. 1–4, Jul. 2020.

[34] B. Zaluski *et al.*, "Terastream implementation of all IP new architecture," in *Proc. of MIPRO 2013*, pp. 437–440, Sept. 2013.

[35] O. Ayoub, S. Shehata, F. Musumeci, and M. Tornatore, "Filterless and semi-filterless solutions in a metro-HAUL network architecture," in *Proc. of ICTON 2018*, pp. 1–4, Jul. 2018.

[36] O. Ayoub *et al.*, "Traffic-adaptive re-configuration of programmable filterless optical networks," in *Proc. of ICC 2020*, pp. 1–6, Jul. 2020.

[37] Z. Xu *et al.*, "1+1 dedicated optical-layer protection strategy for filterless optical networks," *IEEE Commun. Lett.*, vol. 18, pp. 98–101, Jan. 2014.

[38] M. Ibrahimi *et al.*, "Strategies for dedicated path protection in filterless optical networks," in *Proc. of GLOBECOM 2021*, pp. 1–6, Dec. 2021.

[39] E. Archambault *et al.*, "Design and simulation of filterless optical networks: problem definition and performance evaluation," *J. Opt. Commun. Netw.*, vol. 2, pp. 495–501, Jul. 2010.

[40] C. Tremblay *et al.*, "Passive filterless core networks based on advanced modulation and electrical compensation technologies," *Telecommun. Syst.*, vol. 54, pp. 167–181, Jul. 2013.

[41] Z. Xu *et al.*, "Flexible bandwidth allocation in filterless optical networks," *IEEE Commun. Lett.*, vol. 19, pp. 565–568, Apr. 2015.

[42] O. Ayoub, A. Bovio, F. Musumeci, and M. Tornatore, "Survivable virtual network mapping with fiber tree establishment in filterless optical networks," *IEEE Trans. Netw. Serv. Manag.*, pp. 37–48, Sept. 2021.

[43] B. Jaumard, Y. Wang, and D. Coudert, "DantzigWolfe decomposition for the design of filterless optical networks," *J. Opt. Commun. Netw.*, vol. 13, pp. 312–321, Sept. 2021.

[44] B. Jaumard, Y. Wang, and N. Huin, "Optimal design of filterless optical networks," in *Proc. of ICTON 2018*, pp. 1–5, Jul. 2018.

[45] G. Mantelet *et al.*, "Establishment of dynamic lightpaths in filterless optical networks," *J. Opt. Commun. Netw.*, vol. 5, pp. 312–321, Sept. 2013.

[46] M. Garey and D. Johnson, *Computers and Intractability: a Guide to the Theory of NP-Completeness*. W. H. Freeman & Co. New York, 1979.

[47] E. Archambault *et al.*, "Routing and spectrum assignment in elastic filterless optical networks," *IEEE/ACM Trans. Netw.*, vol. 24, pp. 3578–3592, Dec. 2016.

[48] E. Balas, M. Manfred, and R. Peeters, "Set partitioning: A survey," *SIAM Rev.*, vol. 18, pp. 710–760, Oct. 1976.

[49] N. Young, "Randomized rounding without solving the linear program," in *Proc. of SODA 2002*, pp. 170–178, May 2002.

[50] P. Raghavan and C. Tompson, "Randomized rounding: a technique for provably good algorithms and algorithmic proofs," *Combinatorica*, vol. 7, pp. 365–374, Dec. 1987.

[51] B. Nikhil, "On a generalization of iterated and randomized rounding," in *Proc. of STOC 2019*, pp. 1125–1135, Jun. 2019.

[52] "Linear Programming." [Online]. Available: https://en.wikipedia.org/wiki/Linear_programming.

[53] "Gurobi." [Online]. Available: https://www.gurobi.com/.